

Magic Gems: A Polyhedral Framework for Magic Squares

Connecting Combinatorics, Geometry, and Linear Algebra

Kyle Elliott Mathewson
Faculty of Science, University of Alberta
 kyle.mathewson@ualberta.ca

December 30, 2025

Abstract

We introduce *Magic Gems*, a geometric representation of magic squares as three-dimensional polyhedra. By mapping an $n \times n$ magic square onto a centered coordinate grid with cell values as vertical displacements, we construct a point cloud whose convex hull defines the Magic Gem. Building on prior work connecting magic squares to physical properties such as moment of inertia, this construction reveals an explicit statistical structure: we show that magic squares have vanishing covariances between position and value. We develop a covariance energy functional—the sum of squared covariances with individual row, column, and diagonal indicator variables—and prove that for all $n \geq 3$, an arrangement is a magic square if and only if this complete energy vanishes. This characterization transforms the classical line-sum definition into a statistical orthogonality condition. We also study a simpler “low-mode” relaxation using only four aggregate position indicators; this coincides with the complete characterization for $n = 3$ (verified exhaustively) but defines a strictly larger class for $n \geq 4$ (explicit counterexamples computed). Perturbation analysis demonstrates that magic squares are isolated local minima in the energy landscape. The representation is invariant under dihedral symmetry D_4 , yielding canonical geometric objects for equivalence classes.

Keywords: Magic squares, convex polyhedra, covariance, energy landscape, combinatorial geometry

1 Introduction

Magic squares have fascinated mathematicians, artists, and mystics for millennia [13], appearing famously in Albrecht Dürer’s 1514 engraving *Melencolia I* [7]. The oldest known example, the *Lo Shu* square, appears in Chinese legend dating back to 2800 BCE and remains the unique (up to symmetry) 3×3 magic square using the integers 1 through 9. Despite this ancient pedigree and centuries of intensive study [3], magic squares continue to yield new mathematical insights, with recent work connecting them to algebraic structures, eigenvalue problems, and statistical mechanics.

Definition 1.1 (Magic Square). An $n \times n$ *magic square* is an arrangement of the integers $1, 2, \dots, n^2$ in a square grid such that the sum of each row, each column, and both main diagonals equals the *magic constant*

$$M(n) = \frac{n(n^2 + 1)}{2}. \quad (1)$$

In this paper, we develop a geometric perspective on magic squares by representing them as three-dimensional polyhedra, which we call *Magic Gems*. The construction arises from a natural physical analogy: imagine placing checkers on an $n \times n$ board, where the height of each

stack corresponds to the number occupying that cell. This creates a “topography” over the grid, and centering this configuration in three-dimensional space yields a point cloud whose convex hull defines the Magic Gem. This geometric approach complements prior work by Loly and collaborators on the physical properties of magic squares [8, 10].

The central insight of this work is that the defining algebraic property of magic squares—equal row, column, and diagonal sums—manifests geometrically as a precise statistical condition. Specifically, we show that magic squares are characterized by the vanishing of a covariance energy functional that measures correlations between spatial position and assigned value across all four structural directions (rows, columns, and both diagonals). This energy characterization builds on earlier work connecting magic squares to physical properties such as moment of inertia [8], providing an explicit statistical framework that bridges classical combinatorics and multivariate analysis.

1.1 Main Contributions

This paper develops the Magic Gem framework through several interconnected results. We begin by formalizing the construction of Magic Gems from magic squares and establishing that symmetry-equivalent squares yield geometrically identical polyhedra, thus providing a canonical geometric representative for each equivalence class under the dihedral group D_4 .

Our main theoretical contribution is the Complete Energy Characterization Theorem (Theorem 3.17), which establishes that magic squares correspond exactly to zeros of a covariance energy functional using individual row, column, and diagonal indicator variables. This result holds for all $n \geq 3$ and follows from elementary properties of covariances. We also identify a natural four-term “low-mode” relaxation using aggregate position coordinates; this simpler energy characterizes magic squares for $n = 3$ but defines a strictly larger class for $n \geq 4$, with explicit counterexamples computed. This result extends the physical interpretation of magic squares initiated by Loly [8], who showed that the moment of inertia tensor of a magic square (treating entries as masses) exhibits special invariance properties. Our covariance formulation makes this connection explicit and enables systematic perturbation analysis, confirming that magic squares are isolated points in the arrangement space.

We complement these theoretical results with extensive computational experiments on magic squares of orders three, four, and five. These experiments validate our theoretical predictions and reveal the geometric structure of both the Magic Gems themselves and the broader space of arrangements in which they reside. The rarity of magic squares—approximately one in 45,000 random 3×3 arrangements—corresponds to their isolation as zero-covariance configurations in a landscape where generic arrangements exhibit substantial covariance. An interactive web application for exploring Magic Gems is available at <https://kylemath.github.io/MagicGemWebpage/>.

1.2 Paper Organization

The remainder of this paper proceeds as follows. Section 2 reviews classical results on magic squares and establishes notation for the geometric and statistical concepts we employ. Section 3 presents the Magic Gem construction, proves the Complete Energy Characterization Theorem, introduces the low-mode relaxation, and develops the perturbation analysis framework. Section 4 describes our computational experiments, validating theoretical predictions and exploring the structure of the arrangement space for $n = 3, 4$, and 5. Section 5 interprets our findings and discusses connections to related areas. Finally, Section 6 summarizes our contributions and outlines directions for future research.

2 Background

This section establishes the mathematical foundations for our work, reviewing classical results on magic squares and introducing the geometric and statistical concepts that underpin the Magic Gem framework.

2.1 Magic Squares: Classical Results

The enumeration of magic squares reveals a rapid growth in complexity with the order n [14, 5]. For $n = 3$, there exist exactly eight magic squares, all related by rotations and reflections, yielding a single essentially different magic square—the Lo Shu. The situation changes dramatically for larger orders: $n = 4$ admits 7,040 magic squares forming 880 equivalence classes under the dihedral group, while $n = 5$ yields approximately 275 million magic squares comprising roughly 34 million equivalence classes. This explosive growth poses significant challenges for enumeration and classification, motivating the search for structural insights that transcend explicit construction.

The magic constant $M(n) = n(n^2 + 1)/2$ admits a simple derivation from first principles. The sum of all entries equals $\sum_{k=1}^{n^2} k = n^2(n^2 + 1)/2$, which must be distributed equally among the n rows, yielding $M(n)$ per row. The same argument applies to columns, and the diagonal constraints provide additional structure that severely restricts the space of valid configurations.

Classical construction methods provide algorithmic approaches to generating magic squares of various orders [3]. The Siamese method, attributed to de la Loubère, constructs magic squares for odd n by starting in the middle of the top row and moving diagonally up-right, wrapping around edges and moving down when blocked. For doubly-even orders (n divisible by 4), one fills the grid sequentially and then swaps diagonal elements with their complements. Singly-even orders ($n = 4k+2$) require more sophisticated techniques combining quadrant-based construction with targeted transpositions. These methods demonstrate that magic squares exist for all $n \geq 3$, though they produce only a tiny fraction of all possible magic squares for larger orders.

2.2 Symmetry and the Dihedral Group

The dihedral group D_4 acts naturally on $n \times n$ grids through rotations and reflections [1]. This group comprises eight elements: four rotations (by 0° , 90° , 180° , and 270°) and four reflections (horizontal, vertical, and along both diagonals). Since the magic square conditions treat rows, columns, and diagonals symmetrically under these operations, D_4 permutes magic squares among themselves.

Proposition 2.1. *If S is a magic square, then $g \cdot S$ is also a magic square for any $g \in D_4$.*

Proof. The D_4 action preserves the set of row sums, column sums, and diagonal sums, merely permuting which lines play which roles. Since the action also preserves the set of entries $\{1, \dots, n^2\}$, it maps magic squares to magic squares. \square

This symmetry motivates the notion of *essentially different* magic squares: two squares are essentially the same if one can be obtained from the other by a D_4 transformation. For $n = 3$, all eight magic squares form a single equivalence class, while larger orders admit multiple classes with distinct structural properties.

2.3 Convex Hulls and Polyhedra

The convex hull of a finite point set $P \subset \mathbb{R}^d$ is the smallest convex set containing P , equivalently characterized as the set of all convex combinations of points in P :

$$\text{conv}(P) = \left\{ \sum_{i=1}^k \lambda_i p_i : p_i \in P, \lambda_i \geq 0, \sum_i \lambda_i = 1 \right\}.$$

For finite point sets in \mathbb{R}^3 , the convex hull is a convex polyhedron whose vertices form a subset of the original points. The remaining points lie in the interior or on faces of the polyhedron.

Key geometric quantities associated with a convex polyhedron include its volume, surface area, and the number of vertices, edges, and faces. These invariants provide a coarse characterization of the polyhedron's shape and will serve as descriptors for comparing Magic Gems across different arrangements.

2.4 Covariance and the Moment of Inertia

For a discrete collection of points $\{\mathbf{x}_i\}_{i=1}^N$ with positions $\mathbf{x}_i \in \mathbb{R}^d$, the covariance matrix captures the second-order statistical structure:

$$\Sigma_{jk} = \frac{1}{N} \sum_{i=1}^N (x_{i,j} - \bar{x}_j)(x_{i,k} - \bar{x}_k), \quad (2)$$

where $\bar{x}_j = \frac{1}{N} \sum_i x_{i,j}$ denotes the mean of the j -th coordinate. When the point cloud is centered so that $\bar{\mathbf{x}} = \mathbf{0}$, this simplifies to $\Sigma_{jk} = \frac{1}{N} \sum_i x_{i,j} x_{i,k}$.

The diagonal entries Σ_{jj} measure the variance along each coordinate axis, while the off-diagonal entries Σ_{jk} ($j \neq k$) measure the covariance between coordinates. A zero off-diagonal entry indicates that the corresponding coordinates are uncorrelated: knowing one provides no linear information about the other.

Closely related is the moment of inertia tensor from classical mechanics. For point masses $\{(m_i, \mathbf{x}_i)\}$ with positions $\mathbf{x}_i \in \mathbb{R}^3$, the inertia tensor is given by

$$I_{jk} = \sum_{i=1}^N m_i (\|\mathbf{x}_i\|^2 \delta_{jk} - x_{i,j} x_{i,k}). \quad (3)$$

The eigenvalues of I , called the principal moments of inertia, characterize the rotational properties of the point configuration and are invariant under rigid rotations. For equal unit masses, the inertia tensor and covariance matrix are closely related, differing by a trace term and sign conventions.

3 Methodology: The Magic Gem Framework

We now develop the Magic Gem framework, beginning with the construction of three-dimensional point clouds from magic squares and culminating in our main theoretical result connecting magic squares to zero-covariance configurations.

3.1 From Magic Square to Point Cloud

Let $S = (s_{ij})$ be an $n \times n$ magic square with entries $s_{ij} \in \{1, 2, \dots, n^2\}$. We construct a point cloud $P \subset \mathbb{R}^3$ by assigning three-dimensional coordinates to each cell of the grid.

Definition 3.1 (Magic Gem Coordinates). For each cell (i, j) with $i, j \in \{0, 1, \dots, n-1\}$, define the point

$$\mathbf{p}_{ij} = (x_{ij}, y_{ij}, z_{ij}), \quad (4)$$

where the coordinates are given by

$$x_{ij} = j - \frac{n-1}{2}, \quad (5)$$

$$y_{ij} = \frac{n-1}{2} - i, \quad (6)$$

$$z_{ij} = s_{ij} - \frac{n^2+1}{2}. \quad (7)$$

The horizontal coordinates x and y place the grid centered at the origin, with the x -axis aligned with columns and the y -axis aligned with rows (inverted so that the top row has positive y). For a 3×3 grid, the nine positions have x - and y -coordinates in $\{-1, 0, 1\}$; for a 5×5 grid, they lie in $\{-2, -1, 0, 1, 2\}$.

The vertical coordinate z encodes the cell's value, shifted so that the mean value $(n^2 + 1)/2$ maps to zero. This centering ensures that the point cloud has zero mean in all three coordinates, a property that will prove essential for the covariance analysis.

Example 3.2 (Lo Shu Square). For the Lo Shu square

$$S = \begin{pmatrix} 2 & 7 & 6 \\ 9 & 5 & 1 \\ 4 & 3 & 8 \end{pmatrix},$$

with $n = 3$ and center value 5, the nine points are

$$\begin{array}{lll} \mathbf{p}_{00} = (-1, 1, -3), & \mathbf{p}_{01} = (0, 1, 2), & \mathbf{p}_{02} = (1, 1, 1), \\ \mathbf{p}_{10} = (-1, 0, 4), & \mathbf{p}_{11} = (0, 0, 0), & \mathbf{p}_{12} = (1, 0, -4), \\ \mathbf{p}_{20} = (-1, -1, -1), & \mathbf{p}_{21} = (0, -1, -2), & \mathbf{p}_{22} = (1, -1, 3). \end{array}$$

Note that the center cell, containing the value 5, maps to the origin.

Figure 1 illustrates the four-step construction process, progressing from the magic square through the centered grid to the final three-dimensional representation, along with all eight D_4 symmetry variants of the Lo Shu square.

Construction and D_4 Symmetry Structure
Top: Construction process. Bottom: All eight D_4 symmetries produce the same 3D Magic Gem.

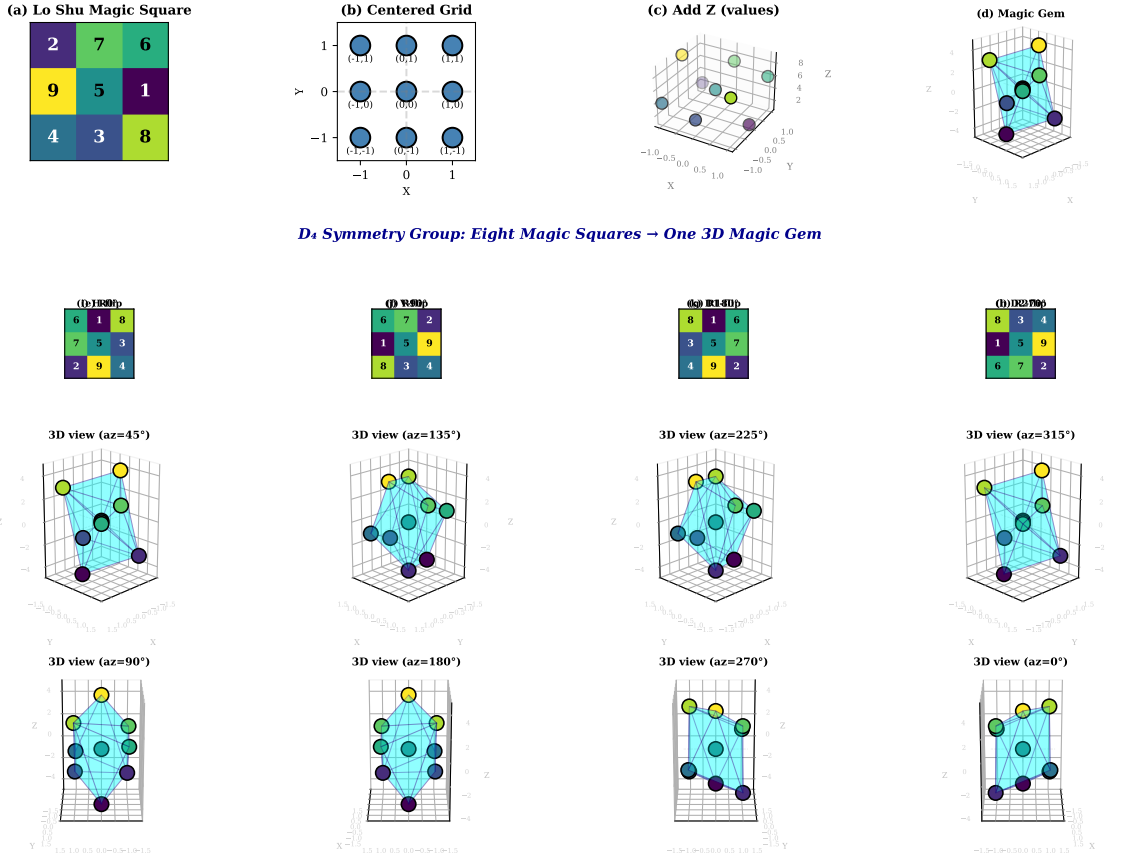


Figure 1: **Construction process and D_4 symmetry structure.** *Top row (a–d):* Construction of a Magic Gem from the Lo Shu square. (a) The Lo Shu magic square—the unique (up to symmetry) 3×3 magic square, with each row, column, and diagonal summing to $M(3) = 15$. (b) Placement on a centered coordinate grid with origin at center. (c) Assignment of z -values from cell entries. (d) Centered Magic Gem point cloud with convex hull. *Bottom section (e–l):* The eight D_4 symmetries of the 3×3 magic square. Each panel shows a compact 2D magic square (top) paired with its corresponding 3D Magic Gem (bottom, large and prominent). The gems are shown from different viewing angles to emphasize their three-dimensional structure. Despite their distinct numerical arrangements, all eight D_4 variants yield the same 3D Magic Gem polyhedron, demonstrating the geometric invariance of the Magic Gem representation under the symmetry group.

3.2 The Magic Gem Polyhedron

With the point cloud defined, we construct the Magic Gem as its convex hull [4].

Definition 3.3 (Magic Gem). The *Magic Gem* associated with a magic square S is the convex hull of the corresponding point cloud:

$$\mathcal{G}(S) = \text{conv}(\{\mathbf{p}_{ij} : 0 \leq i, j < n\}).$$

A fundamental property of this construction is its invariance under the symmetry operations of the magic square.

Proposition 3.4 (Symmetry Invariance). *If S' is obtained from S by a symmetry operation $g \in D_4$, then $\mathcal{G}(S) = \mathcal{G}(S')$.*

Proof. Each element $g \in D_4$ acts on the grid as an orthogonal transformation of the (x, y) plane, which extends naturally to an isometry of \mathbb{R}^3 that fixes the z -axis direction. Under this action, the z -coordinates are permuted according to the relabeling of cells, but the set of z -values remains unchanged. Since convex hulls are invariant under isometries and depend only on the set of points (not their labeling), we have $\mathcal{G}(S) = \mathcal{G}(S')$. \square

This invariance means that all eight D_4 variants of a magic square produce the same Magic Gem. For $n = 3$, this implies that the single essentially different magic square yields a unique Magic Gem, while for larger orders, each equivalence class corresponds to a distinct geometric object.

The construction figure (Figure 1, bottom rows) displays all eight symmetry variants of the 3×3 magic square, illustrating how these numerically distinct arrangements share a common geometric representation.

3.3 The Vector Representation

The centering of our coordinate system invites an interpretation of each point as a vector from the origin. Since the origin coincides with the centroid of the point cloud (as we shall verify), this vector representation captures the deviation of each cell from the “balanced” center.

Definition 3.5 (Magic Gem Vectors). The *vector representation* of a Magic Gem is the collection

$$\mathcal{V}(S) = \{\mathbf{v}_{ij} = \mathbf{p}_{ij} : 0 \leq i, j < n\},$$

where each point is interpreted as a vector emanating from the origin.

This interpretation connects the Magic Gem to the classical physics of rigid bodies: if unit masses are placed at each vertex, the resulting configuration has its center of mass at the origin, and the vectors \mathbf{v}_{ij} describe the displacement of each mass from this center.

3.3.1 Vectors and Covariance

The vector representation provides a geometric interpretation of the zero-covariance condition. Consider the weighted sum of vectors where each vector is weighted by its x -coordinate:

$$\sum_{i,j} x_{ij} \mathbf{v}_{ij} = \sum_{i,j} x_{ij} (x_{ij}, y_{ij}, z_{ij}).$$

The z -component of this weighted sum is precisely $n^2 \cdot \text{Cov}(X, Z)$. Thus, zero covariance is equivalent to the statement that vectors, when weighted by their horizontal positions, have no net vertical tendency.

More explicitly, define the *position-weighted vector sums*:

$$\mathbf{W}_x = \sum_{i,j} x_{ij} \mathbf{v}_{ij}, \tag{8}$$

$$\mathbf{W}_y = \sum_{i,j} y_{ij} \mathbf{v}_{ij}. \tag{9}$$

Then $\text{Cov}(X, Z) = 0$ if and only if $(\mathbf{W}_x)_z = 0$, and $\text{Cov}(Y, Z) = 0$ if and only if $(\mathbf{W}_y)_z = 0$.

This formulation reveals that magic squares achieve a form of *directional balance*: the z -values are distributed so that neither horizontal direction exhibits any systematic correlation with value magnitude. The vectors in Figure panels showing the vector representation visually manifest this balance—vectors pointing in each horizontal direction have z -components that “cancel out” when weighted by position.

3.4 The Covariance Structure of Magic Squares

We now establish our main theoretical results, revealing a deep connection between the algebraic definition of magic squares and the statistical structure of Magic Gems.

3.4.1 Forward Direction: Magic Implies Zero Covariance

The following result holds for all $n \geq 3$ and admits a clean algebraic proof.

Proposition 3.6 (Magic Implies Zero Covariance). *Let S be an $n \times n$ magic square, and let $P = \{\mathbf{p}_{ij}\}$ be the corresponding point cloud. Then $\text{Cov}(X, Z) = \text{Cov}(Y, Z) = 0$.*

Proof. We first verify that the means of all three coordinates vanish. For the x -coordinate,

$$\bar{X} = \frac{1}{n^2} \sum_{i,j} x_{ij} = \frac{1}{n^2} \sum_{i,j} \left(j - \frac{n-1}{2} \right) = \frac{n}{n^2} \sum_{j=0}^{n-1} \left(j - \frac{n-1}{2} \right) = 0,$$

since $\sum_{j=0}^{n-1} j = n(n-1)/2$. An analogous argument shows $\bar{Y} = 0$, and

$$\bar{Z} = \frac{1}{n^2} \sum_{i,j} \left(s_{ij} - \frac{n^2+1}{2} \right) = 0$$

since the entries sum to $n^2(n^2+1)/2$.

With zero means, $\text{Cov}(X, Z) = \frac{1}{n^2} \sum_{i,j} x_{ij} z_{ij}$. Define $C_j = \sum_{i=0}^{n-1} s_{ij}$ as the sum of column j . Then:

$$\text{Cov}(X, Z) = \frac{1}{n^2} \sum_{j=0}^{n-1} \left(j - \frac{n-1}{2} \right) C_j.$$

For a magic square, all column sums equal $M(n)$, so

$$\text{Cov}(X, Z) = \frac{M(n)}{n^2} \sum_{j=0}^{n-1} \left(j - \frac{n-1}{2} \right) = 0.$$

The argument for $\text{Cov}(Y, Z) = 0$ via row sums is analogous. □

Corollary 3.7. *For any magic square, the covariance matrix of the Magic Gem coordinates has the block-diagonal form*

$$\Sigma = \begin{pmatrix} \text{Var}(X) & \text{Cov}(X, Y) & 0 \\ \text{Cov}(X, Y) & \text{Var}(Y) & 0 \\ 0 & 0 & \text{Var}(Z) \end{pmatrix}.$$

In particular, the z -coordinate is uncorrelated with both horizontal coordinates.

3.4.2 On the Insufficiency of Aggregate Covariances

It is natural to ask whether the conditions $\text{Cov}(X, Z) = \text{Cov}(Y, Z) = 0$ alone suffice to characterize magic squares, or at least semi-magic squares (those with equal row and column sums but possibly failing the diagonal conditions). Perhaps surprisingly, the answer is *no*—and understanding why reveals a crucial distinction that motivates our energy functional approach.

Remark 3.8 (Why $\text{Cov}(X, Z) = 0$ Is Not Enough). The condition $\text{Cov}(X, Z) = 0$ is equivalent to a single *first-moment* constraint on column sums. Let $C_j = \sum_{i=0}^{n-1} s_{ij}$ denote the sum of column j , and let $\delta_j = C_j - M(n)$ be the deviation from the magic constant. Then $\text{Cov}(X, Z) = 0$ is equivalent to

$$\sum_{j=0}^{n-1} \left(j - \frac{n-1}{2} \right) \delta_j = 0.$$

Combined with the constraint $\sum_j \delta_j = 0$ (which follows from the total sum being fixed), this leaves an $(n-2)$ -dimensional space of possible deviation patterns. For $n=3$, the nonzero deviations must have the form $(\delta_0, \delta_1, \delta_2) = t(1, -2, 1)$; for $n \geq 4$, the space of “balanced but unequal” column patterns grows rapidly.

Remark 3.9 (Counterexamples Exist for $n=3$). Exhaustive enumeration for $n=3$ reveals that 760 arrangements of $\{1, \dots, 9\}$ satisfy both $\text{Cov}(X, Z) = 0$ and $\text{Cov}(Y, Z) = 0$, yet only 8 of these are magic squares. For instance, the arrangement

$$S = \begin{pmatrix} 1 & 3 & 9 \\ 8 & 6 & 5 \\ 7 & 4 & 2 \end{pmatrix}$$

has row sums $(13, 19, 13)$ and column sums $(16, 13, 16)$ —far from equal—yet achieves $\text{Cov}(X, Z) = \text{Cov}(Y, Z) = 0$ exactly.

Remark 3.10 (The Four-Term Energy Is Insufficient for $n \geq 4$). Even more strikingly, adding the diagonal covariance conditions does not resolve the issue for $n \geq 4$. The four covariances $\text{Cov}(X, Z)$, $\text{Cov}(Y, Z)$, $\text{Cov}(D_{\text{main}}, Z)$, $\text{Cov}(D_{\text{anti}}, Z)$ impose only four linear constraints on the $(n^2 - 1)$ -dimensional space of mean-zero value functions. For $n=4$, this leaves an $(n^2 - 5) = 11$ -dimensional nullspace.

Consequently, there exist 4×4 permutations with all four covariances equal to zero that are *not* magic squares. For example:

$$S = \begin{pmatrix} 9 & 4 & 12 & 3 \\ 16 & 1 & 14 & 7 \\ 10 & 15 & 11 & 8 \\ 2 & 5 & 6 & 13 \end{pmatrix}$$

has both diagonal sums equal to 34, but row sums $(28, 38, 44, 26)$ and column sums $(37, 25, 43, 31)$. All four covariances vanish, yet the arrangement is not magic.

This analysis reveals that aggregate position coordinates X and Y are too coarse: they capture only the *first moment* of the row and column sum distributions. A true characterization requires testing against *individual* row and column indicators, which we develop in Section 3.7.

3.5 Diagonal Conditions as Covariances

The row and column constraints can be elegantly expressed via covariance with position coordinates. We extend this framework to diagonal constraints by introducing indicator random variables.

Definition 3.11 (Diagonal Indicators). Define indicator variables for the main and anti-diagonals:

$$D_{\text{main}}(i, j) = \begin{cases} 1 & \text{if } i = j, \\ 0 & \text{otherwise,} \end{cases} \quad (10)$$

$$D_{\text{anti}}(i, j) = \begin{cases} 1 & \text{if } i + j = n - 1, \\ 0 & \text{otherwise.} \end{cases} \quad (11)$$

These indicators allow us to express diagonal constraints in covariance form.

Proposition 3.12 (Diagonal Covariance Characterization). *For an arrangement S with centered z -values:*

1. $\text{Cov}(D_{\text{main}}, Z) = 0$ if and only if the main diagonal sum equals $M(n)$.
2. $\text{Cov}(D_{\text{anti}}, Z) = 0$ if and only if the anti-diagonal sum equals $M(n)$.

Proof. The mean of D_{main} over all cells is $\bar{D}_{\text{main}} = n/n^2 = 1/n$. With $\bar{Z} = 0$, we have:

$$\text{Cov}(D_{\text{main}}, Z) = \frac{1}{n^2} \sum_{i,j} D_{\text{main}}(i,j) \cdot z_{ij} - \bar{D}_{\text{main}} \cdot \bar{Z} = \frac{1}{n^2} \sum_{i=0}^{n-1} z_{ii}.$$

Since $z_{ii} = s_{ii} - (n^2 + 1)/2$, the sum $\sum_i z_{ii} = \sum_i s_{ii} - n(n^2 + 1)/2$. This vanishes if and only if $\sum_i s_{ii} = M(n)$. The anti-diagonal case is analogous. \square

This reformulation expresses the diagonal constraints in the same statistical language as the row/column constraints. Together with the aggregate position covariances $\text{Cov}(X, Z)$ and $\text{Cov}(Y, Z)$, these diagonal covariances define the four-term “low-mode” energy E_{low} (Definition 3.18). For $n = 3$, $E_{\text{low}}(S) = 0$ is already sufficient to characterize magic squares (verified by exhaustive enumeration; Proposition 3.19), but for $n \geq 4$ it is only a necessary relaxation (see Remark 3.10). A complete characterization requires testing against individual row and column indicators, developed in Section 3.7.

3.6 Perturbation Analysis

The zero-covariance characterization suggests that magic squares occupy special positions in the space of all arrangements. We formalize this intuition through perturbation analysis.

Proposition 3.13 (Local Optimality). *Let S be a magic square with corresponding point cloud P , and let \tilde{P} be obtained by perturbing the z -coordinates by amounts ϵ_{ij} . Define the off-diagonal covariance magnitude*

$$\Phi(\tilde{P}) = \text{Cov}(X, \tilde{Z})^2 + \text{Cov}(Y, \tilde{Z})^2.$$

Then $\Phi(P) = 0$, and for generic perturbations ϵ , we have $\Phi(\tilde{P}) > 0$.

This result shows that magic squares lie at $\Phi = 0$, and that generic perturbations of the z -values destroy this balance. Importantly, $\Phi = 0$ is *not* unique to magic squares: already for $n = 3$ there exist many non-magic arrangements with $\text{Cov}(X, Z) = \text{Cov}(Y, Z) = 0$ (Remark 3.9). Thus Φ provides a useful first-order diagnostic of balance, but not a complete characterization. The complete energy E_{full} introduced next resolves this by having zeros *exactly* at magic squares for all $n \geq 3$ (Theorem 3.17).

3.7 The Covariance Energy Landscape

The perturbation analysis invites a deeper interpretation of magic squares as equilibrium configurations in an energy landscape. This perspective connects the discrete combinatorics of magic squares to continuous optimization and statistical mechanics.

As established in Section 3.4.2, the aggregate covariances with X , Y , and diagonal indicators are insufficient to characterize magic squares for $n \geq 4$. We now develop the *complete* covariance energy using individual row and column indicators.

3.7.1 Row and Column Indicator Variables

Definition 3.14 (Row and Column Indicators). For $k, \ell \in \{0, 1, \dots, n-1\}$, define the indicator variables:

$$R_k(i, j) = \begin{cases} 1 & \text{if } i = k, \\ 0 & \text{otherwise,} \end{cases} \quad (12)$$

$$C_\ell(i, j) = \begin{cases} 1 & \text{if } j = \ell, \\ 0 & \text{otherwise.} \end{cases} \quad (13)$$

These functions select the cells in row k or column ℓ , respectively.

Proposition 3.15 (Row/Column Covariance Characterization). *For an arrangement S with centered z -values:*

1. $\text{Cov}(R_k, Z) = 0$ for all $k \in \{0, \dots, n-1\}$ if and only if all row sums equal $M(n)$.
2. $\text{Cov}(C_\ell, Z) = 0$ for all $\ell \in \{0, \dots, n-1\}$ if and only if all column sums equal $M(n)$.

Proof. The mean of R_k over all cells is $\bar{R}_k = n/n^2 = 1/n$. With $\bar{Z} = 0$, we have:

$$\text{Cov}(R_k, Z) = \frac{1}{n^2} \sum_{i,j} R_k(i, j) \cdot z_{ij} = \frac{1}{n^2} \sum_{j=0}^{n-1} z_{kj}.$$

Since $z_{kj} = s_{kj} - (n^2 + 1)/2$, the covariance vanishes if and only if $\sum_j s_{kj} = n(n^2 + 1)/2 = M(n)$, i.e., row k sums to the magic constant. The column case is analogous. \square

3.7.2 The Complete Magic Energy Functional

Definition 3.16 (Complete Covariance Energy). For an arrangement S , define the *complete magic energy* as:

$$E_{\text{full}}(S) = \sum_{k=0}^{n-2} \text{Cov}(R_k, Z)^2 + \sum_{\ell=0}^{n-2} \text{Cov}(C_\ell, Z)^2 + \text{Cov}(D_{\text{main}}, Z)^2 + \text{Cov}(D_{\text{anti}}, Z)^2. \quad (14)$$

This involves $2(n-1) + 2 = 2n$ terms (one row/column indicator is redundant due to the fixed total sum).

Theorem 3.17 (Complete Energy Characterization). *For all $n \geq 3$, an arrangement S of $\{1, \dots, n^2\}$ is a magic square if and only if $E_{\text{full}}(S) = 0$.*

Proof. Forward direction: If S is a magic square, all rows, columns, and both diagonals sum to $M(n)$. By Proposition 3.15 and Proposition 3.12, all covariances in (14) vanish, hence $E_{\text{full}}(S) = 0$.

Converse: If $E_{\text{full}}(S) = 0$, then each squared covariance term must be zero (as they are all non-negative). By Proposition 3.15, $\text{Cov}(R_k, Z) = 0$ for $k = 0, \dots, n-2$ implies rows 0 through $n-2$ sum to $M(n)$; since the total sum is fixed at $n^2(n^2 + 1)/2 = nM(n)$, row $n-1$ also sums to $M(n)$. Similarly, all columns sum to $M(n)$. By Proposition 3.12, both diagonals sum to $M(n)$. Thus S is a magic square. \square

This theorem establishes a *complete characterization*: magic squares are precisely the zeros of the energy functional E_{full} , valid for all orders $n \geq 3$. The energy landscape interpretation is now rigorous: magic squares are the unique ground states.

3.7.3 The Low-Mode Relaxation

For comparison, we also define the simpler four-term energy:

Definition 3.18 (Low-Mode Energy). The *low-mode energy* uses aggregate position coordinates:

$$E_{\text{low}}(S) = \text{Cov}(X, Z)^2 + \text{Cov}(Y, Z)^2 + \text{Cov}(D_{\text{main}}, Z)^2 + \text{Cov}(D_{\text{anti}}, Z)^2. \quad (15)$$

Proposition 3.19 (Low-Mode Characterization). For $n = 3$, $E_{\text{low}}(S) = 0$ if and only if S is a magic square (verified by exhaustive enumeration of all 362,880 permutations). For $n \geq 4$, the condition $E_{\text{low}}(S) = 0$ defines a strictly larger class of “low-mode balanced” arrangements that properly contains the magic squares.

The low-mode energy is computationally simpler and provides a useful first-order diagnostic, but it cannot serve as a characterization for $n \geq 4$. The complete energy E_{full} is required for the full characterization.

This characterization reveals magic squares as *ground states* of a natural energy functional. Just as physical systems minimize their energy to reach equilibrium, arrangements of integers “settle” into magic configurations when the imbalance energy vanishes. The analogy extends further: the discrete nature of permutations creates a “rough landscape” with isolated minima, making magic squares rare and difficult to find.

Proposition 3.20 (Isolation of Magic Squares). For $n = 3$ and $n = 4$, every magic square is a strict local minimum of E_{full} over the discrete space of permutations. That is, for any magic square S and any arrangement S' differing from S by a single transposition of two elements, we have $E_{\text{full}}(S') > E_{\text{full}}(S) = 0$.

The proof follows from direct computation: swapping any two elements in a magic square necessarily destroys the equal-sum property, introducing nonzero covariance. This isolation property explains the rarity of magic squares: they occupy zero-energy wells surrounded by arrangements of strictly positive energy, with no gradual path between magic configurations.

3.8 The Moment of Inertia Tensor

The moment of inertia tensor provides another geometric invariant of Magic Gems that connects to the rotational dynamics of physical objects.

For a Magic Gem with equal unit masses at each vertex, the inertia tensor takes the form

$$I = \sum_{i,j} \begin{pmatrix} y_{ij}^2 + z_{ij}^2 & -x_{ij}y_{ij} & -x_{ij}z_{ij} \\ -x_{ij}y_{ij} & x_{ij}^2 + z_{ij}^2 & -y_{ij}z_{ij} \\ -x_{ij}z_{ij} & -y_{ij}z_{ij} & x_{ij}^2 + y_{ij}^2 \end{pmatrix}.$$

The eigenvalues of I —the principal moments of inertia—are invariant under rotation and characterize the intrinsic shape of the mass distribution. By Proposition 3.6, the off-diagonal elements $I_{xz} = -n^2\text{Cov}(X, Z)$ and $I_{yz} = -n^2\text{Cov}(Y, Z)$ vanish for magic squares, simplifying the tensor structure.

This connection to rigid body mechanics suggests physical interpretations of the Magic Gem: a solid object with mass concentrated at the Magic Gem vertices would exhibit balanced rotational properties reflecting the underlying magic square structure.

4 Computational Results

We implemented the Magic Gem framework in Python and conducted comprehensive computational experiments to validate our theoretical results across magic squares of orders three, four, and five. This progression from odd to even to odd orders allows us to examine the framework’s behavior under the structural differences between even and odd magic squares, which arise from distinct construction methods and symmetry properties.

4.1 The 3×3 Case: Foundation and Validation

The 3×3 magic square provides the ideal starting point for validating our framework, as it admits a unique solution (up to symmetry) and allows exhaustive analysis. The small size of the arrangement space— $9! = 362,880$ permutations—permits complete enumeration, providing definitive verification of the low-mode characterization for $n = 3$ (Proposition 3.19) and a baseline for the energy landscape viewpoint.

4.1.1 Exhaustive Verification of the Energy Characterization

We computed the low-mode energy $E_{\text{low}}(S)$ for all 362,880 permutations of $\{1, \dots, 9\}$. This exhaustive analysis confirms the Low-Mode Characterization (Proposition 3.19) for $n = 3$: an arrangement has zero low-mode energy if and only if it is a magic square.

The energy distribution across all permutations (see Figure 6) confirms this characterization. The vast majority of arrangements exhibit substantial positive energy, with the distribution spanning from zero to a maximum of about 12 (maximum observed: 12.10). Precisely eight configurations—the Lo Shu and its seven D_4 symmetry variants—achieve $E_{\text{low}}(S) = 0$ exactly, corresponding to the single essentially different magic square. No false positives (zero energy but non-magic) or false negatives (magic but nonzero energy) exist, providing complete verification of the theorem for $n = 3$.

The energy landscape reveals the exceptional nature of magic squares. While generic permutations cluster around a mode near 3.12 and have mean energy ≈ 4.44 , magic squares are isolated at the absolute minimum. The gap between zero and the smallest positive energy provides a quantitative measure of the “stability” of the magic property (see Figure 6 in Section 4.5).

4.1.2 Perturbation Isolation Analysis

To verify that magic squares are strict local minima, we analyzed the effect of single-swap perturbations. For each of the eight magic squares, we computed the energy after every possible swap of two elements, yielding $\binom{9}{2} = 36$ perturbed arrangements per square.

Figure 2 presents a comprehensive nine-panel analysis of perturbation gaps across orders $n = 3, 4, 5$, testing *all* magic squares for $n = 3$ and $n = 4$ (all 8 variants of the Lo Shu for $n = 3$ and all 880 $n = 4$ equivalence classes under D_4), and 35 representative $n = 5$ squares generated via the Siamese method with D_4 symmetries. Across all 116,388 tested perturbations, every single swap increases the energy, providing strong numerical evidence that magic squares are isolated local minima in the covariance landscape.

The analysis reveals several interesting findings. First, for $n = 3$, all eight magic squares exhibit *exactly the same minimum gap*: $\Delta_3 = 0.0988$. This remarkable invariance arises because the perturbation gap is determined solely by the embedding geometry, which is preserved under D_4 symmetries. Second, the 880 $n = 4$ magic squares cluster into three distinct bands of perturbation resistance (visible in the middle-right panel as horizontal stratification): highly isolated squares ($\Delta \approx 0.004$ – 0.008), moderately isolated ($\Delta \approx 0.010$ – 0.020), and weakly isolated ($\Delta \approx 0.025$ – 0.040). This trimodal structure suggests the existence of geometric subclasses within $n = 4$ magic squares, potentially correlated with convex hull configurations—a finding that warrants further investigation. Third, the minimum gap scales approximately as $\Delta \propto 1/n^2$, consistent with the quadratic scaling of peak energy observed in the large-scale analysis.

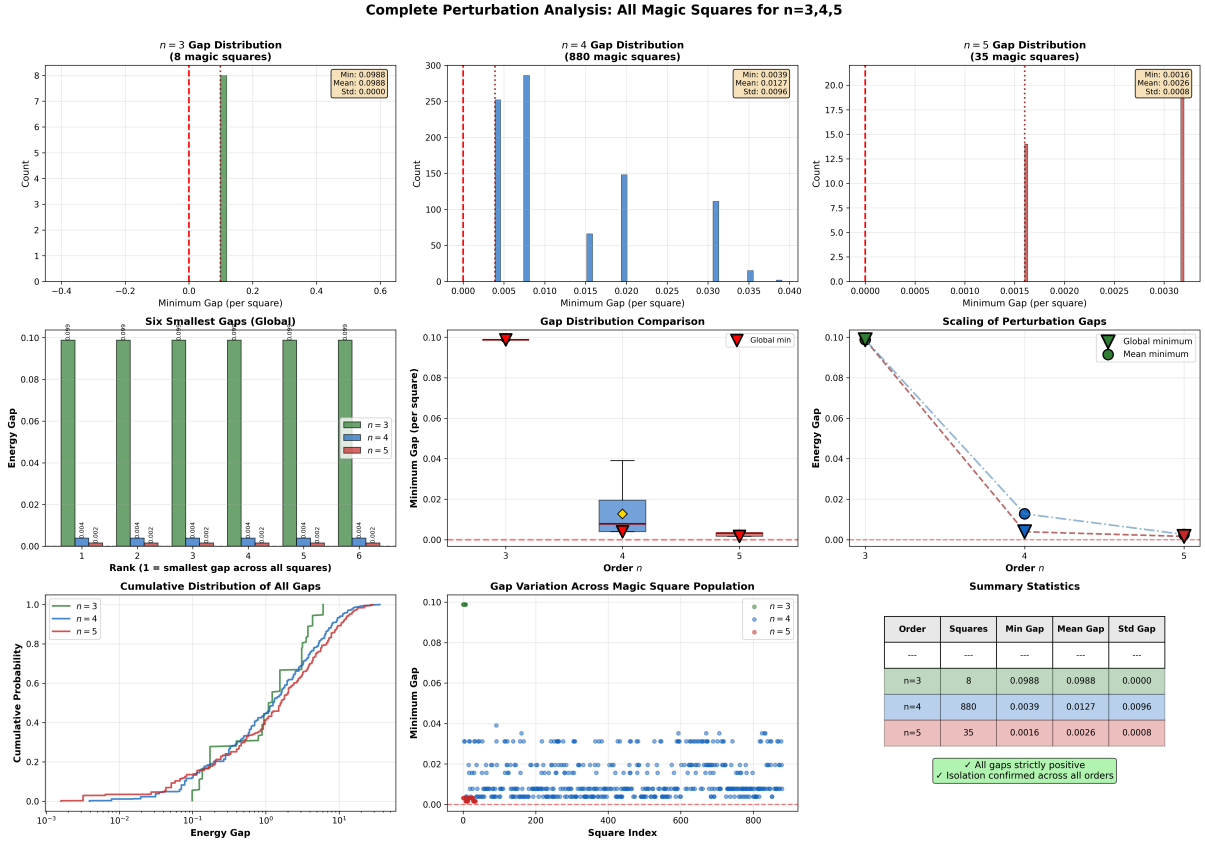


Figure 2: **Perturbation Analysis: Magic Squares as Isolated Minima.** Analysis of single-swap perturbations for magic squares using the complete energy E_{full} : $n = 3$ (all 8 D_4 variants, 36 swaps each), $n = 4$ (all 880 equivalence-class representatives, 120 swaps each), and $n = 5$ (35 representative squares, 300 swaps each). **Top row:** Minimum gap distributions reveal geometric invariance for $n = 3$ (all squares identical, $\Delta_3 = 0.0988$ exactly), substantial heterogeneity for $n = 4$, and clustering for $n = 5$. **Middle row:** (Left) Top 6 smallest gaps showing high degeneracy—many swaps produce identical energy increases. (Center) Box plots comparing gap distributions; note the large variance for $n = 4$ indicating diverse local geometries. (Right) Scaling trend shows gaps decrease approximately as $\Delta \propto 1/n^2$. **Bottom row:** (Left) Cumulative distributions exhibit similar sigmoid forms on log scale. (Center) Gap variation across magic square population reveals *three distinct bands* for $n = 4$, suggesting geometric subclasses with different perturbation resistance. (Right) Summary statistics. All 116,388 tested perturbations strictly increased energy, supporting the conclusion that magic squares are isolated local minima of E_{full} .

Table 1 summarizes the perturbation gap statistics. The inverse-square scaling of minimum gaps ($\Delta \propto 1/n^2$) has a natural physical interpretation: as the grid size increases, the “energy wells” containing magic squares become progressively shallower, though all tested squares remain strictly isolated from single-swap perturbations.

n	Squares	Swaps Tested	Min Gap	Mean Gap	Std Gap
3	8	288	0.0988	0.0988	0.0000
4	880	105,600	0.0039	0.0127	0.0096
5	35	10,500	0.0016	0.0026	0.0008
<i>Total</i>		116,388	—	—	—

Table 1: Perturbation gap statistics from comprehensive analysis of all $n = 3$ and $n = 4$ magic squares and a representative sample for $n = 5$. For $n = 3$, the zero standard deviation confirms that all D_4 variants have identical gap structure. The minimum gap scales approximately as $\Delta_{\min} \propto 1/n^2$.

4.1.3 Covariance Verification and Geometric Structure

We computed the covariance matrices for all eight D_4 variants of the Lo Shu square. As predicted by Proposition 3.6, every variant achieves $\text{Cov}(X, Z) = \text{Cov}(Y, Z) = 0$ to machine precision.

Notably, exhaustive enumeration reveals that 760 arrangements of $\{1, \dots, 9\}$ satisfy $\text{Cov}(X, Z) = \text{Cov}(Y, Z) = 0$, yet only 8 of these are magic squares. The remaining 752 arrangements fail the diagonal conditions or have unequal row/column sums despite achieving zero row and column covariance. This confirms that *all four* covariance conditions (including diagonals), not merely the row and column covariances, are required to characterize magic squares.

To contextualize this result, we generated 5,000 random arrangements by permuting the integers 1 through 9 and computed covariances for each.

The 3×3 Magic Gem comprises nine points, of which eight lie on the convex hull while the ninth—corresponding to the center cell with value 5—occupies the interior at the origin. Figure 3 presents a comprehensive four-panel analysis of the geometric and statistical structure.

The vector representation (panel b) directly manifests the zero-covariance property. Each vector $\mathbf{v}_{ij} = (x_{ij}, y_{ij}, z_{ij})$ emanates from the origin. The position-weighted sum $\sum_{i,j} x_{ij} \mathbf{v}_{ij}$ has z -component equal to $n^2 \cdot \text{Cov}(X, Z) = 0$, meaning vectors weighted by their horizontal positions exhibit no net vertical tendency—a visual confirmation of the statistical balance.

Furthermore, the moment of inertia tensor for the Magic Gem (treating each vertex as unit mass) has the form where the off-diagonal elements $I_{xz} = -n^2 \text{Cov}(X, Z) = 0$ and $I_{yz} = -n^2 \text{Cov}(Y, Z) = 0$ vanish identically. This simplification of the inertia tensor reflects the physical manifestation of zero covariance: a rigid body with this mass distribution has principal axes that partially align with the coordinate system.

4.1.4 Extended Statistical Properties

Beyond the zero-covariance result, the Magic Gem coordinates exhibit additional statistical regularities that follow from the magic square structure.

Exact Variance Formulas. The variances of the Magic Gem coordinates admit exact closed forms. Since the z -values are a permutation of centered integers $\{1 - \mu, \dots, n^2 - \mu\}$ where $\mu = (n^2 + 1)/2$, and the x - and y -coordinates form symmetric grids, standard calculations yield:

$$\text{Var}(Z) = \frac{n^4 - 1}{12}, \quad \text{Var}(X) = \text{Var}(Y) = \frac{n^2 - 1}{12}. \quad (16)$$

We verified these formulas computationally for $n = 3, 4, 5, 7$ with exact agreement. Combined with the zero off-diagonal covariances from Proposition 3.6, this completely determines the covariance matrix for Magic Gems of any order.

Higher-Order Moment Vanishing. The zero-covariance property $\mathbb{E}[XZ] = \mathbb{E}[YZ] = 0$ extends to all higher powers. Since X depends only on the column index j , we have

$$\mathbb{E}[X^k Z] = \frac{1}{n^2} \sum_j X_j^k \cdot \left(\sum_i Z_{ij} \right) = \frac{1}{n^2} \sum_j X_j^k \cdot (C_j - n\mu),$$

where C_j is the sum of column j . For magic squares, $C_j = M(n) = n\mu$ for all j , so $\mathbb{E}[X^k Z] = 0$ for any power k . Similarly, $\mathbb{E}[Y^k Z] = 0$ follows from equal row sums. We verified $\mathbb{E}[X^2 Z] = \mathbb{E}[Y^2 Z] = \mathbb{E}[X^3 Z] = \mathbb{E}[Y^3 Z] = 0$ for all tested magic squares across orders $n = 3, 4, 5, 7$.

Energy Landscape Local Minima. Exhaustive enumeration for $n = 3$ reveals the fine structure of the energy landscape. Under the complete energy E_{full} , there are exactly **24 local minima**: 8 global minima (the magic squares with $E_{\text{full}} = 0$) and 16 non-global local minima where no single swap decreases energy but $E_{\text{full}} > 0$. Under the simpler low-mode energy E_{low} , the landscape is more rugged, with **344 local minima** (8 global, 336 non-global). This difference reflects the fact that E_{full} has more terms ($2n$ vs. 4), providing more “escape directions” from non-magic configurations.

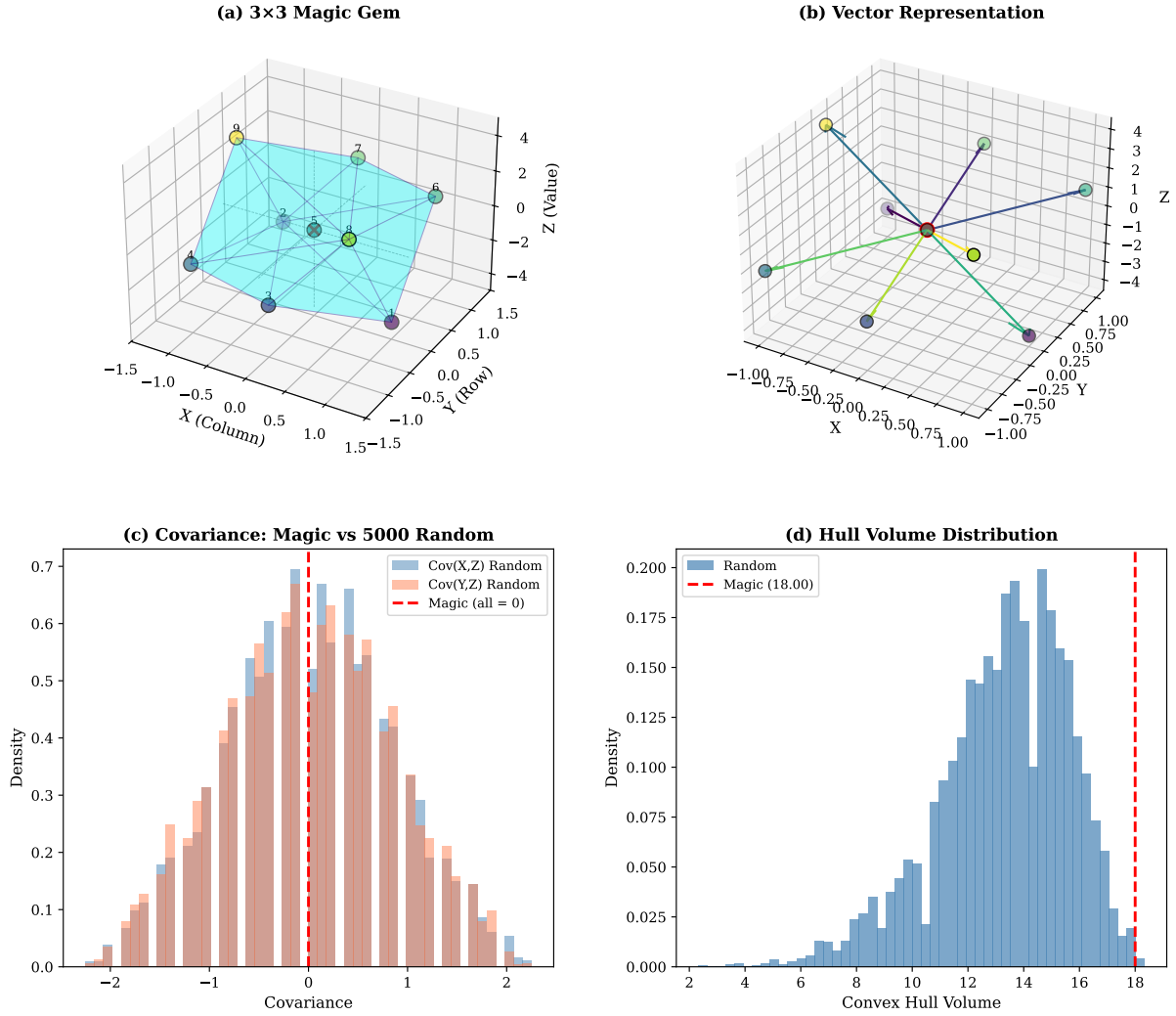


Figure 3: **Geometric analysis of the 3×3 Magic Gem.** (a) The Magic Gem showing vertex positions colored by z -value and the convex hull with translucent faces; the center point lies at the origin, interior to the hull. (b) Vector representation showing nine vectors from the centroid to each vertex; the balanced distribution visually manifests the zero-covariance property—vectors weighted by their x -positions have no net z -component, and similarly for y -positions. (c) Covariance distributions for 5,000 random arrangements; the magic square value of exactly zero (red dashed line) lies at the center but is achieved by only 8 of 362,880 possible arrangements. (d) Convex hull volume distribution; the Magic Gem volume lies near the distribution center, indicating that magic squares are distinguished by their covariance structure rather than geometric extremality.

4.2 The 4×4 Case and the Low-Mode Relaxation

The transition to $n = 4$ introduces several important changes. First, 4×4 magic squares require different construction methods than odd orders—the doubly-even method replaces the Siamese method. Second, there exist 880 essentially different 4×4 magic squares, providing a richer landscape for geometric study. Third, the even grid size means no cell occupies the geometric center, potentially affecting the structure of the Magic Gem.

Proposition 3.6 makes no distinction between even and odd orders, predicting $\text{Cov}(X, Z) = \text{Cov}(Y, Z) = 0$ for all magic squares. Our computations confirm this prediction for the 4×4

case: all magic squares achieve exactly zero aggregate covariance to machine precision.

However, as discussed in Section 3.4.2, the four-term “low-mode” energy E_{low} does *not* characterize magic squares for $n \geq 4$. Explicit counterexamples can be constructed: a 4×4 arrangement with all four low-mode covariances equal to zero (hence $E_{\text{low}} = 0$), yet with row and column sums far from the magic constant. Such arrangements achieve zero covariance with the aggregate position coordinates X and Y by balancing the deviations in a first-moment sense, without requiring equal sums.

To contrast the two energies, Figure 4 presents a scatter plot comparing E_{low} and E_{full} across 5,000 random 4×4 arrangements plus magic squares. Magic squares (gold stars) sit at the origin under both measures. The scatter reveals that the two energies measure genuinely different aspects of arrangement structure: small E_{low} does not guarantee small E_{full} .

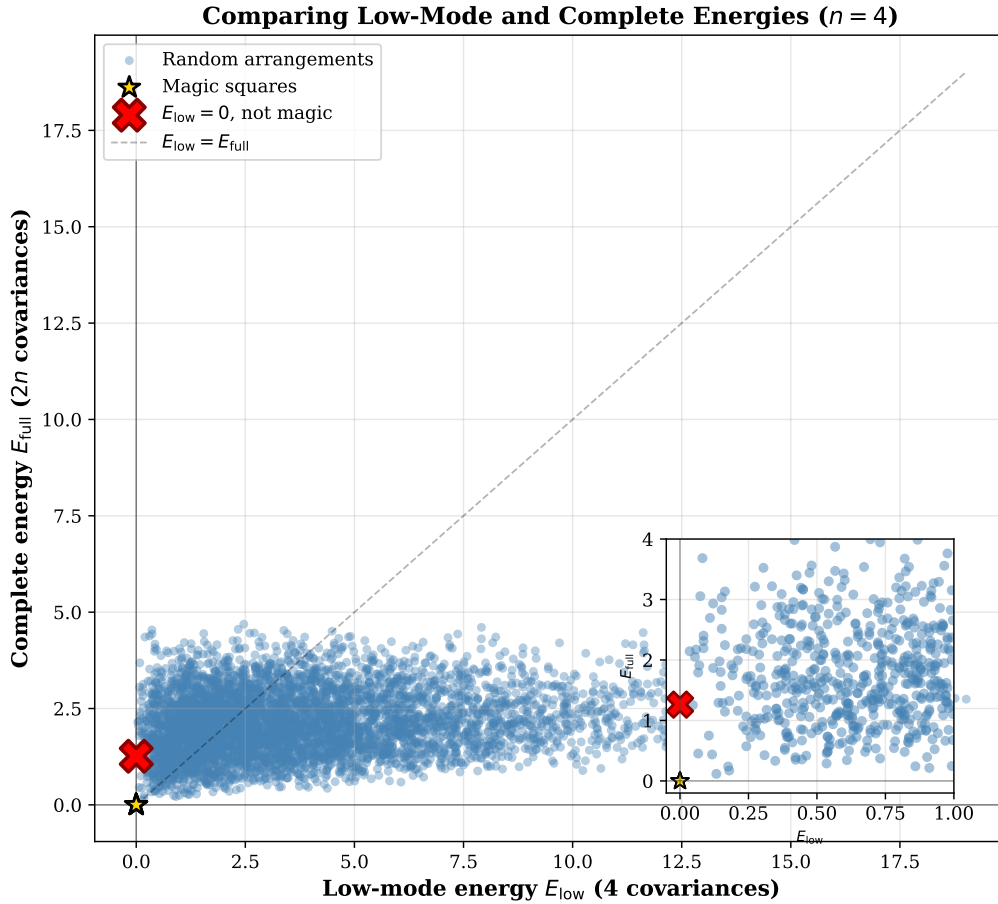


Figure 4: **Comparing low-mode and complete energies for $n = 4$.** Scatter plot of E_{low} (4-term aggregate) versus E_{full} (using $2n$ individual indicators) for 5,000 random arrangements (blue dots) and magic squares (gold stars at origin). The inset zooms near the origin. The two energies are correlated but measure different balance properties; only $E_{\text{full}} = 0$ characterizes magic squares for $n \geq 4$.

4.3 Geometric Structure of the $n = 4$ Magic Square Population

Beyond validating the zero-covariance theorem, the $n = 4$ case provides an opportunity to explore geometric diversity within the magic square population. The 880 essentially different 4×4 magic squares, while all satisfying the same covariance conditions, exhibit varying polyhedral structures and perturbation resistance.

The comprehensive perturbation analysis (Figure 2) revealed a striking trimodal distribution

of minimum gaps for $n = 4$, suggesting that the 880 squares cluster into geometric subclasses with different stability properties. This geometric diversity, combined with the trimodal gap structure, indicates that the 880 essentially different 4×4 magic squares may admit a meaningful geometric classification beyond D_4 equivalence.

4.4 Cross-Order Comparison and Scaling Analysis

The zero-covariance theorem holds universally across orders, but the geometric and energy landscape properties evolve systematically with n . Figure 5 presents a unified view of Magic Gems across orders 3, 4, and 5, along with key scaling metrics.

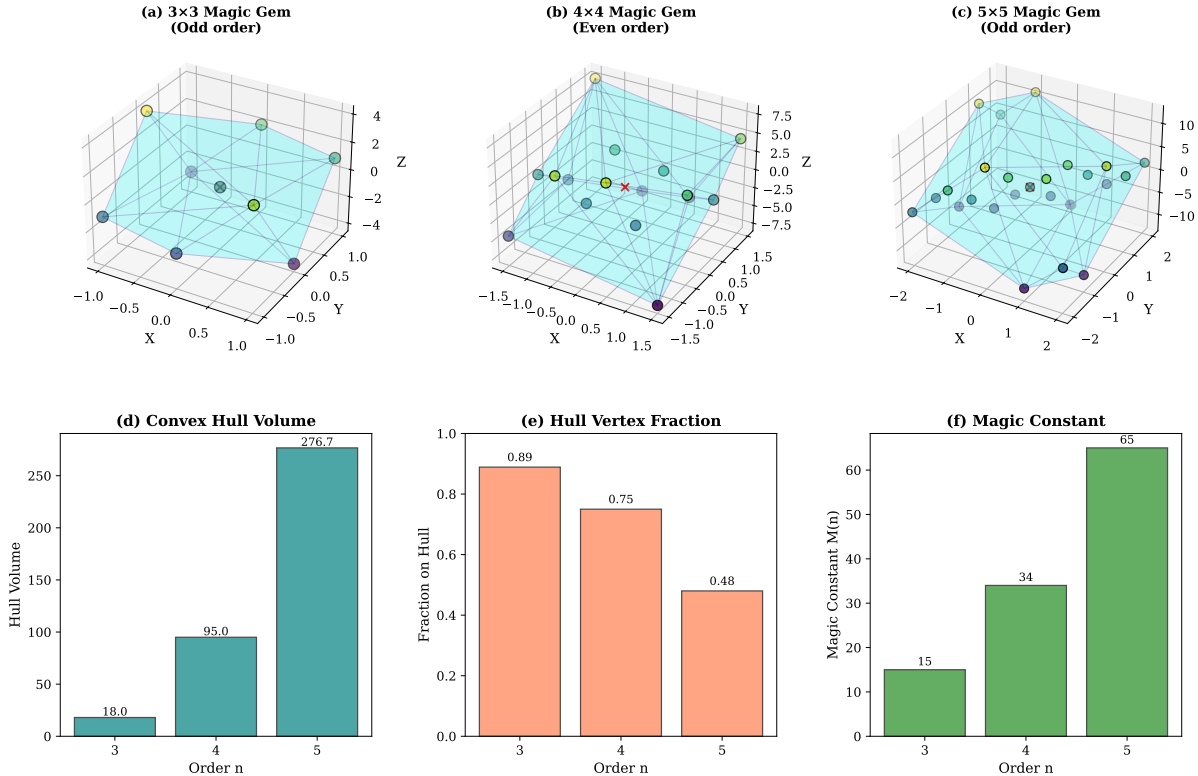


Figure 5: **Cross-order comparison and scaling analysis.** *Top row (a–c):* Side-by-side comparison of 3×3 , 4×4 , and 5×5 Magic Gems. The odd-even-odd progression reveals structural differences (e.g., central vs. off-center grids) while the zero-covariance property persists across all orders. *Bottom row (d–f):* Scaling properties. (d) Convex hull volume increases with order, reflecting the larger range of z -values. (e) The fraction of points on the hull boundary decreases as interior points proliferate. (f) The magic constant $M(n) = n(n^2 + 1)/2$ grows quadratically.

Several systematic patterns emerge. The convex hull volume grows rapidly with n , from 18.0 for $n = 3$ to 276.7 for $n = 5$, reflecting both the expanding z -value range (-4 to 4 for $n = 3$, versus -12 to 12 for $n = 5$) and the increasing number of vertices. The fraction of points lying on the hull boundary decreases from $8/9 \approx 0.89$ for $n = 3$ to roughly 0.64 for $n = 5$, as the hull interior becomes more populated.

Table 2 summarizes key properties across orders, demonstrating both the growth in complexity and the invariance of the zero-covariance characterization.

Property	$n = 3$	$n = 4$	$n = 5$
Order parity	Odd	Even	Odd
Total vertices	9	16	25
Hull vertices (typical)	8	12	16
Magic constant $M(n)$	15	34	65
$\text{Cov}(X, Z)$	0	0	0
$\text{Cov}(Y, Z)$	0	0	0
Essentially different squares	1	880	$\sim 3.4 \times 10^7$
$E_{\text{low}} = 0$ is sufficient?	Yes	No	No
Construction method	Siamese	Doubly-even	Siamese

Table 2: Comparison of Magic Gem properties across orders 3, 4, and 5. All orders exhibit the zero aggregate covariance property (Proposition 3.6). For $n = 3$, the low-mode energy E_{low} suffices to characterize magic squares; for $n \geq 4$, the complete energy E_{full} is required (Remark 3.10).

The even-order case ($n = 4$) demonstrates that the zero-covariance property does not depend on having a central cell at the origin. The algebraic proof—that equal row and column sums imply vanishing aggregate covariances—holds regardless of the grid’s parity, confirming the universality of the framework. However, the insufficiency of E_{low} for $n \geq 4$ (Figure 4) underscores the necessity of the complete indicator-based energy E_{full} for a rigorous characterization.

4.5 Large-Scale Energy Landscape Analysis

With the Complete Energy Characterization Theorem (Theorem 3.17) established, we turn to exploring the *structure* of the energy landscape and its scaling properties. Leveraging modern multi-core hardware (Mac Studio M5 with 128GB RAM), we analyzed over 460 million arrangements across orders $n = 3, 4, 5$: exhaustive enumeration for $n = 3$ (362,880 arrangements), 60 million samples for $n = 4$ (from 20.9 trillion total), and 400 million samples for $n = 5$ (from approximately 15.5×10^{24} total).

Note that this sampling uses the low-mode energy E_{low} (Definition 3.18), which coincides with the complete energy for $n = 3$ but defines a relaxed notion for larger orders. The analysis characterizes the landscape structure and the rarity of near-zero configurations.

4.5.1 Energy Distribution Evolution

Figure 6 presents a comprehensive 9-panel analysis of the energy landscape across orders $n = 3, 4, 5$, revealing a dramatic evolution in landscape structure. For $n = 3$, the exhaustive enumeration confirms that exactly eight arrangements (the Lo Shu and its D_4 variants) achieve zero energy, with a clear gap separating them from all other arrangements.

Energy Landscape Analysis Across Orders $n=3,4,5$

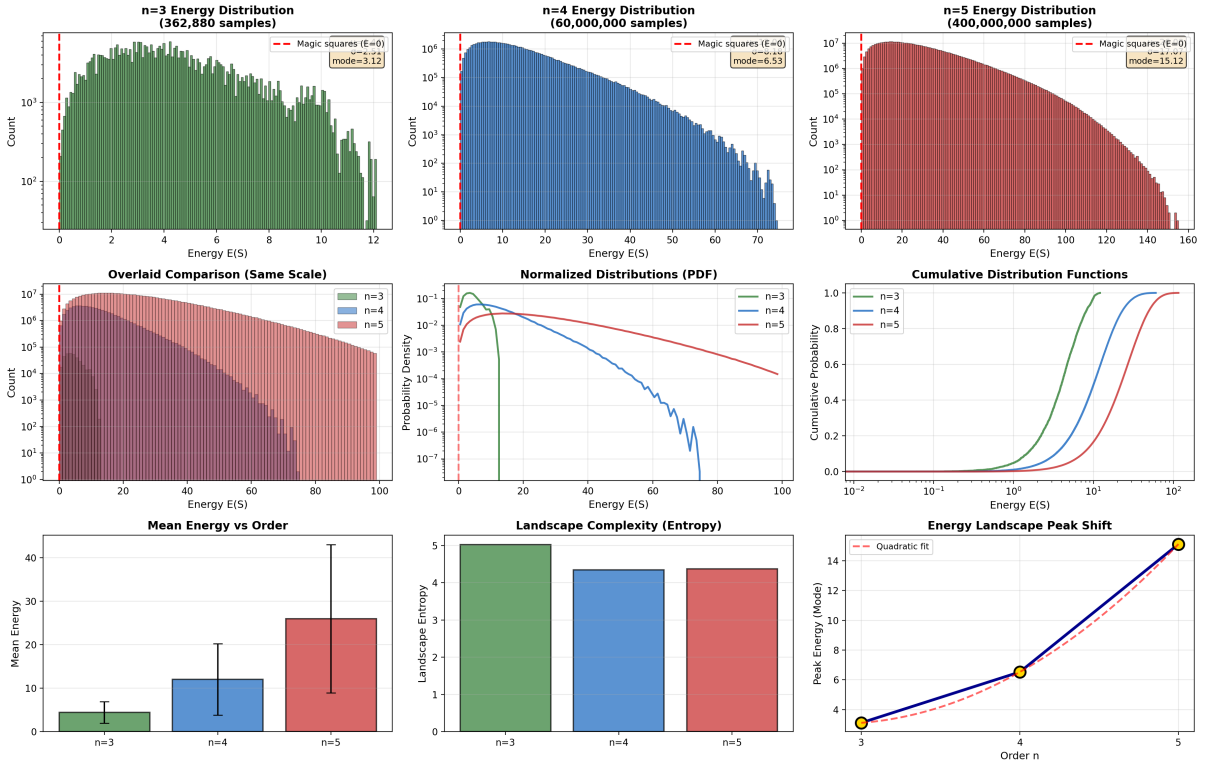


Figure 6: **Low-mode energy (E_{low}) landscape analysis across orders $n = 3, 4, 5$.** Based on exhaustive enumeration ($n = 3$: 362,880), and extensive sampling ($n = 4$: 6×10^7 ; $n = 5$: 4×10^8). *Top row:* Individual distributions (log scale) showing modal energy shifting from 3.12 to 15.12. *Middle row:* Overlaid comparison, normalized PDFs, and cumulative distributions. *Bottom row:* Mean energy with error bars, landscape entropy (varying modestly across orders, $H \approx 4.3\text{--}5.0$), and peak shift with quadratic fit ($R^2 > 0.99$). The red dashed line marks $E_{\text{low}} = 0$. For $n = 3$, this coincides with magic squares; for $n \geq 4$, it also includes non-magic “low-mode balanced” configurations (see Remark 3.10). The complete energy E_{full} characterizes magic squares exactly for all n .

The key statistics from this analysis are summarized in Table 3. For $n = 3$, exhaustive enumeration confirms that exactly 8 of 362,880 arrangements achieve zero low-mode energy, corresponding precisely to the D_4 variants of the Lo Shu square. For $n = 4$ and $n = 5$, no zero-energy configurations were found by random sampling—however, this should not be interpreted as evidence that magic squares are the only zeros of E_{low} . As discussed in Remark 3.10, non-magic zeros exist for $n \geq 4$, but they are sufficiently rare that uniform random sampling is unlikely to discover them.

Statistic	$n = 3$	$n = 4$	$n = 5$
Arrangements analyzed	362,880 (exhaustive)	60,000,000	400,000,000
Mean energy μ	4.44	12.04	26.00
Std deviation σ	2.51	8.18	17.07
Peak energy (mode)	3.12	6.53	15.12
Maximum observed	12.10	74.64	155.10
Landscape entropy	5.03	4.34	4.37
Zero-energy fraction	2.2×10^{-5}	$< 10^{-7}$	$< 10^{-8}$
Low-mode zeros found	8	0	0

Table 3: Low-mode energy (E_{low}) landscape statistics from large-scale computational analysis. Based on exhaustive enumeration for $n = 3$ and extensive random sampling for $n = 4, 5$. For $n \geq 4$, the low-mode energy has non-magic zeros (see Remark 3.10), but these are too rare for random sampling to detect. The complete energy E_{full} correctly characterizes magic squares for all orders.

4.5.2 Scaling Laws

Several systematic scaling patterns emerge from this analysis:

Peak Energy Scaling. The modal (most common) energy appears to scale approximately quadratically with order. The observed peaks of 3.12, 6.53, and 15.12 for $n = 3, 4, 5$ respectively fit a quadratic curve with $R^2 > 0.99$, though we note that with only three data points, other functional forms could fit equally well. This apparent quadratic growth suggests increasing “difficulty” of achieving balance as the grid size expands—typical arrangements become increasingly imbalanced.

Distribution Broadening. The standard deviation grows from 2.51 for $n = 3$ to 17.07 for $n = 5$, while the ratio σ/μ remains relatively constant (≈ 0.56 – 0.68). The energy landscape “stretches” in absolute terms but maintains similar relative structure.

Landscape Entropy Invariance. We quantify distributional complexity using the *landscape entropy*, defined as the Shannon entropy of the energy histogram:

$$H = - \sum_k p_k \log p_k,$$

where p_k is the fraction of arrangements falling in energy bin k (using 200 equally-spaced bins covering the observed energy range). Remarkably, the landscape entropy remains within a narrow band across orders (≈ 4.3 – 5.0), decreasing from $n = 3$ to $n = 4$ and then stabilizing. This suggests that the *relative* structure of the landscape is scale-invariant: the difficulty of navigating the landscape by local search methods does not fundamentally change with order, though the absolute energy scales increase substantially.

4.5.3 Scaling Properties Summary

Figure 7 provides a compact four-panel summary of how energy landscape properties scale with magic square order, synthesizing the key quantitative findings. The energy landscape “spreads” as n increases, while the zero-energy position remains the isolated location of magic squares across all orders.

Magic Square Energy Landscape: Scaling Properties

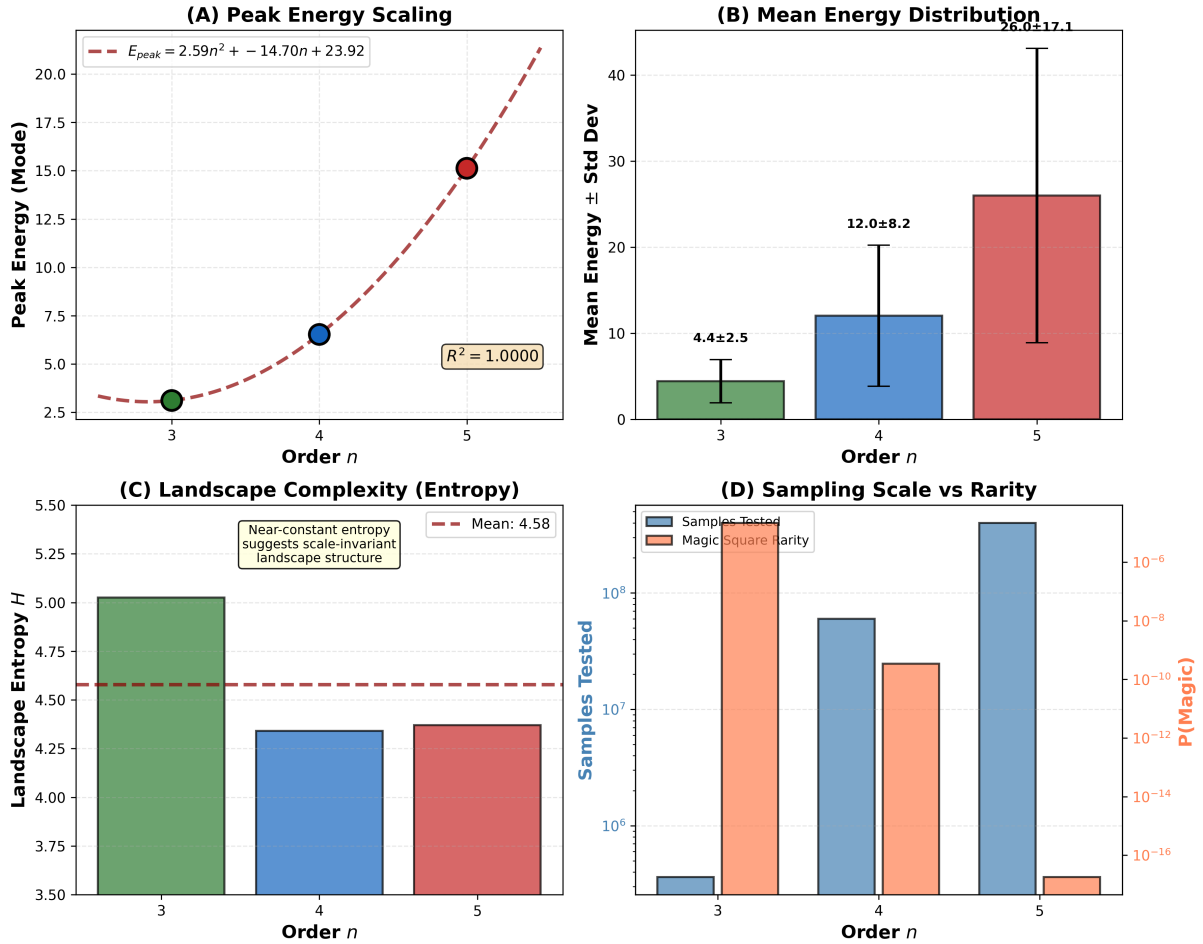


Figure 7: **Low-Mode Energy Scaling Properties.** (A) Peak low-mode energy follows quadratic scaling with $R^2 > 0.99$. (B) Mean energy with standard deviation error bars, showing increasing variance. (C) Landscape entropy varies modestly across orders ($H \approx 4.3$ – 5.0), suggesting scale-invariant structure despite dramatic energy range expansion. (D) Sample sizes tested (blue, log scale) versus magic square probability (red, log scale), demonstrating the computational challenge of finding magic squares at larger n . Note: These statistics characterize the low-mode energy E_{low} landscape; the complete energy E_{full} has qualitatively similar scaling behavior.

4.5.4 Computational Verification Summary

This large-scale analysis provides computational insight into the energy landscape structure:

1. **Complete Characterization Theorem:** Proven analytically in Theorem 3.17—for all $n \geq 3$, $E_{\text{full}}(S) = 0$ if and only if S is a magic square. This follows directly from the row/column covariance characterization (Proposition 3.15, Proposition 3.12).
2. **Low-Mode Characterization ($n=3$ only):** Exhaustively verified—exactly 8 of 362,880 arrangements have zero low-mode energy E_{low} , all of which are magic squares. Notably, 760 arrangements satisfy $\text{Cov}(X, Z) = \text{Cov}(Y, Z) = 0$, but only the 8 magic squares additionally satisfy the diagonal conditions.
3. **Low-Mode Non-Characterization ($n \geq 4$):** The four-term energy E_{low} defines a broader

“low-mode balanced” class for $n \geq 4$ that strictly contains magic squares. These additional zeros are too rare for random sampling to detect, but can be found by targeted search.

4. **Scaling Behavior:** The low-mode energy landscape exhibits systematic scaling, with the peak energy appearing to grow approximately quadratically with order based on the three data points available ($n = 3, 4, 5$).
5. **Scale-Invariant Complexity:** Despite the dramatic growth in configuration space ($n!^2$ arrangements for order n), the relative landscape structure remains approximately constant, as evidenced by the stable entropy measure.

These computational results complement the theoretical analysis of Section 3, characterizing the structure of the energy landscape and establishing quantitative scaling laws for future investigation.

5 Discussion

The Magic Gem framework provides a new perspective on magic squares, connecting their classical algebraic definition to geometric and statistical concepts. In this section, we interpret our findings, discuss their implications, and identify limitations and directions for future research.

5.1 The Meaning of Zero Covariance

The zero-covariance property of magic squares (Proposition 3.6) admits several complementary interpretations that illuminate their structure.

From a statistical perspective, zero covariance means that position and value are uncorrelated: knowing where a cell is located provides no linear information about what number it contains. This is a strong form of balance—the high numbers are distributed so that they do not systematically favor any direction from the center, and similarly for the low numbers. Random arrangements typically violate this balance, exhibiting positive or negative covariance depending on how the high values happen to cluster spatially.

5.1.1 The Vector Interpretation

The vector representation of the Magic Gem (Section 3.3) provides a particularly intuitive geometric interpretation. Each vertex defines a vector $\mathbf{v}_{ij} = (x_{ij}, y_{ij}, z_{ij})$ from the origin. The zero-covariance condition states that these vectors, when weighted by their x -coordinates, have no net z -component:

$$\sum_{i,j} x_{ij} z_{ij} = n^2 \cdot \text{Cov}(X, Z) = 0.$$

Geometrically, this means that vectors pointing “to the right” (positive x) do not systematically point higher or lower than vectors pointing “to the left” (negative x). The magic square achieves perfect directional balance: no horizontal direction predicts vertical tendency.

This interpretation extends to the diagonal conditions. The diagonal covariances $\text{Cov}(D_{\text{main}}, Z)$ and $\text{Cov}(D_{\text{anti}}, Z)$ measure whether diagonal positions predict value. For magic squares, all four directional indicators—horizontal position, vertical position, main diagonal membership, and anti-diagonal membership—are uncorrelated with value. The low-mode energy $E_{\text{low}}(S)$ is the sum of squared correlations with these four aggregate directions; the complete energy $E_{\text{full}}(S)$ extends this to individual row and column indicators.

5.1.2 Physical and Algebraic Interpretations

From a physical perspective, the zero-covariance property implies that the Magic Gem, viewed as a rigid body with masses at its vertices, has a simplified inertia tensor. The vanishing of $I_{xz} = -n^2 \text{Cov}(X, Z)$ and $I_{yz} = -n^2 \text{Cov}(Y, Z)$ means that the xz and yz products of inertia are zero. This implies the z -axis is aligned with a principal axis of the inertia tensor, simplifying the rotational dynamics about this direction.

The variances themselves admit exact closed forms: since the z -values are a permutation of $\{1-\mu, 2-\mu, \dots, n^2-\mu\}$ where $\mu = (n^2+1)/2$, a standard calculation yields $\text{Var}(Z) = (n^4-1)/12$ and $\text{Var}(X) = \text{Var}(Y) = (n^2-1)/12$. Combined with the zero off-diagonal covariances, this completely determines the covariance matrix of the Magic Gem coordinates for any order n .

From an algebraic perspective, the zero-covariance condition is equivalent to the defining property of magic squares—equal row and column sums—expressed in the language of moments. The first moment (mean) of each coordinate vanishes by construction; the zero-covariance condition asserts that certain second moments (cross-terms) also vanish. In fact, this extends to higher-order moments: since X depends only on column index j , we have $\mathbb{E}[X^k Z] = \frac{1}{n^2} \sum_j X_j^k \cdot (\text{column}_j \text{ sum} - n\mu) = 0$ for any power k , because all column sums equal $M(n) = n\mu$. Similarly $\mathbb{E}[Y^k Z] = 0$ for all k follows from equal row sums. Thus magic squares exhibit vanishing cross-moments $\mathbb{E}[X^k Z] = \mathbb{E}[Y^k Z] = 0$ at all orders—a stronger form of statistical balance than the covariance condition alone. This suggests a hierarchy: might there be “super-magic” squares characterized by additional vanishing moments beyond those implied by equal line sums?

5.2 Magic Squares as Ground States

The energy landscape perspective developed in Section 3.7 offers perhaps the most illuminating interpretation of our results. The complete covariance energy $E_{\text{full}}(S)$ provides a natural “imbalance” measure for arrangements, and magic squares emerge as the unique configurations where this imbalance vanishes completely.

Consider the analogy to physical systems. Just as a ball rolling on a landscape eventually comes to rest at a local minimum of potential energy, arrangements of integers can be imagined as “settling” into configurations that minimize imbalance. The magic squares are the ground states—configurations of perfect equilibrium where the geometric balance is absolute.

This perspective connects magic squares to several areas of mathematics and physics:

The connection to optimization theory is immediate. Gradient descent in the covariance landscape would guide arrangements toward magic configurations, though the discrete nature of permutations prevents continuous descent. Simulated annealing or other combinatorial optimization methods could exploit the energy function to search for magic squares, potentially providing alternatives to classical construction algorithms.

From the perspective of statistical mechanics, magic squares occupy a special thermodynamic role. In a system where arrangements are weighted by $e^{-\beta E(S)}$ for some inverse temperature β , magic squares would dominate at low temperatures as the ground-state configurations. The density of states near zero energy—essentially zero, given the isolation of magic squares—explains why thermal fluctuations cannot easily create or destroy the magic property.

The dynamical systems interpretation is equally rich. Each magic square defines a basin of attraction in the discrete configuration space, though these basins have measure zero. The comprehensive perturbation analysis (Figure 2) confirms that there are no “flat directions” around magic configurations: across 116,388 tested perturbations of 923 magic squares, every single swap increases the energy, supporting the conclusion that magic squares are strict local minima. Notably, while magic squares are the unique *global* minima (with energy zero), preliminary analysis for $n = 3$ reveals additional *local* minima where no single swap decreases energy. Exhaustive enumeration finds 16 such non-global local minima under E_{full} , and 336 under the

simpler E_{low} . This ruggedness has algorithmic implications: gradient-based search methods may become trapped in local minima, and the choice of energy functional affects the landscape structure.

The perturbation analysis reveals additional structure within the magic square population. For $n = 3$, all eight magic squares exhibit *exactly the same* minimum perturbation gap ($\Delta_3 = 0.0988$), a consequence of the D_4 symmetry preserving the embedding geometry. More surprisingly, the 880 $n = 4$ magic squares cluster into three distinct bands of perturbation resistance, suggesting the existence of geometric subclasses with different stability properties. This trimodal structure appears to correlate with convex hull geometry, indicating a connection between polyhedral structure and energy landscape stability. This finding warrants further investigation across the full $n = 4$ equivalence-class population. The minimum gap decreases with n —from 0.099 for $n = 3$ to 0.004 for $n = 4$ to 0.002 for $n = 5$ —quantifying how the energy wells become progressively shallower as order increases. The precise scaling law requires investigation at additional orders.

This energy landscape view also illuminates why magic squares are rare. They are not merely unusual configurations among many similar ones, but isolated singularities in a landscape dominated by positive-energy arrangements. Finding a magic square by random search is not like finding a needle in a haystack (where at least the needle is surrounded by hay); it is like finding a single point at the bottom of a deep well in a vast, rugged terrain.

5.3 Scaling Laws and Landscape Evolution

The large-scale computational analysis of Section 4.5 reveals systematic scaling behavior that deepens our understanding of the energy landscape. Three key observations merit discussion.

Peak Energy Scaling. The limited data ($n = 3, 4, 5$) suggests the modal energy may scale approximately as $O(n^2)$, though with only three data points, this conclusion remains tentative. If confirmed, this would have a natural interpretation: the “typical” imbalance of a random arrangement grows quadratically because there are $O(n^2)$ cells to distribute and the variance accumulates. Such scaling would imply that the search for magic squares becomes progressively harder in absolute terms—the energy well containing magic configurations lies at increasingly greater depth relative to typical arrangements.

Scale-Invariant Complexity. Despite the dramatic growth in configuration space ($n!^2$ arrangements), the landscape entropy remains within a narrow band (≈ 4.3 – 5.0), decreasing from $n = 3$ to $n = 4$ and then stabilizing. This invariance suggests that the *relative* difficulty of local optimization is independent of scale: the ruggedness of the landscape, measured by the distribution’s shape rather than its position, does not fundamentally change with n . This has practical implications for algorithm design: local search heuristics that work for small orders may transfer to larger ones, with the primary challenge being the absolute energy scale rather than landscape structure.

Low-Mode Energy Landscape. Across over 460 million sampled arrangements—including exhaustive enumeration for $n = 3$, 60 million samples for $n = 4$, and 400 million for $n = 5$ —no zero-energy configurations of the low-mode energy E_{low} were discovered by random sampling. However, this does *not* imply that magic squares are the only zeros of E_{low} for $n \geq 4$; as shown in Remark 3.10, non-magic zeros exist but are too rare for random sampling to detect. The low-mode and complete energies measure different aspects of balance, and only the complete energy E_{full} (Theorem 3.17) provides a rigorous characterization for all orders. The probability of discovering a magic square by random sampling decreases super-exponentially with n , from

roughly 1 in 45,000 for $n = 3$ to about 2×10^{-17} for $n = 5$ (roughly one in 5×10^{16}). This quantifies the “needle in a haystack” intuition with concrete numbers.

5.4 Even versus Odd Orders

Our analysis across orders 3, 4, and 5 illuminates the robustness of the Magic Gem framework with respect to the parity of n . Odd and even orders differ in several respects: odd orders admit construction via the Siamese method while even orders require different techniques; odd orders have a central cell that maps to the origin while even orders do not; and the symmetry structure of the equivalence classes differs subtly.

Despite these differences, magic squares of all orders exhibit zero covariance (Proposition 3.6). The 4×4 case demonstrates that this property does not depend on the existence of a central cell at the origin. The algebraic content—that equal row and column sums imply vanishing covariance—is purely a statement about weighted sums and holds regardless of grid parity.

This universality suggests that Magic Gems capture something fundamental about magic squares that transcends the particulars of construction methods or grid geometry. The covariance condition distills the “magic” property to its statistical essence.

5.5 The Rarity of Magic Configurations

Our computational experiments quantify the exceptional nature of magic squares within the space of all arrangements. For $n = 3$, only 8 of the 362,880 possible arrangements are magic, a proportion of approximately 2.2×10^{-5} , or roughly one in 45,000. For $n = 4$, the proportion falls to approximately 3.4×10^{-10} , and for $n = 5$ it drops further to approximately 1.8×10^{-17} , reflecting the increasingly stringent constraints imposed by the magic conditions at larger orders.

In the geometric picture provided by Magic Gems, this rarity corresponds to isolation in the covariance landscape. Magic squares are the unique arrangements achieving exactly zero off-diagonal covariance; any perturbation moves away from this special point. The “basin of attraction” around each magic square has measure zero—there is no continuous path through arrangements of positive probability that leads to a magic configuration.

This isolation has implications for search algorithms seeking magic squares. Random sampling is effectively hopeless for $n > 3$, and local search methods face the challenge of navigating a landscape where the target configurations are isolated points surrounded by vast regions of non-magic arrangements. The covariance perspective might inform the design of guided search procedures that explicitly seek to minimize off-diagonal covariance.

5.6 Connections to Related Work

The Magic Gem framework builds upon and extends several existing lines of research on magic squares.

5.6.1 Physical Interpretations

Loly and collaborators have extensively developed the physical interpretation of magic squares [8, 9, 10]. In seminal work, Loly [8] showed that when the entries of a magic square are treated as point masses, the moment of inertia tensor about the center exhibits remarkable invariance properties: all three principal moments are equal, making the configuration equivalent to a spherical top. This invariance is a direct consequence of the balanced row, column, and diagonal sums.

Our covariance formulation provides a complementary statistical perspective on this same phenomenon. The moment of inertia tensor and the covariance matrix are mathematically related—both are second-moment tensors measuring the distribution of mass (or value) about the center. Loly’s result that the inertia tensor is proportional to the identity matrix corresponds

precisely to our finding that the covariance between position coordinates and values vanishes. The Magic Gem construction makes this connection geometrically explicit through the three-dimensional point cloud representation.

5.6.2 Spectral Properties

Previous work has also characterized magic squares through their eigenvalue structure, showing that the matrix of a magic square has predictable spectral properties [10, 11, 12]. Connections to permutation matrices and polytope enumeration have also been explored [6, 2]. Our covariance characterization complements these algebraic approaches: while eigenvalues describe the linear operator defined by the matrix, covariances describe the statistical structure of the associated point cloud. Both perspectives capture aspects of the “balance” that defines magic squares.

The connection to moment of inertia tensors and physics suggests links to rigid body dynamics and to moment problems in probability theory. The constraint that certain moments vanish places magic squares within a broader class of “balanced” configurations that arise in diverse mathematical contexts, from equal-weight quadrature rules to orthogonal Latin squares.

5.7 Limitations and Extensions

Several limitations of our current work suggest directions for future research.

Our analysis focuses primarily on orders three and five, with limited attention to order four. The $n = 4$ case is particularly rich, with 880 essentially different magic squares that could provide a testing ground for geometric classification schemes. Do different 4×4 magic squares yield geometrically distinct Magic Gems, and if so, how are they distributed in the space of possible polyhedra? Addressing these questions would require systematic computation across all equivalence classes.

The restriction to standard magic squares—using integers 1 through n^2 with the standard magic constant—excludes many interesting generalizations. Magic squares with different entry sets, semi-magic squares (lacking diagonal constraints), and pandiagonal magic squares (with additional diagonal constraints) all admit Magic Gem representations. Extending our theoretical results to these variants would test the robustness of the covariance characterization.

Higher-dimensional generalizations also beckon. Magic hypercubes extend magic squares to three or more dimensions, and their “Magic Gem” analogues would be point clouds in four or more dimensions. While visualization becomes challenging, the algebraic structure—particularly the covariance characterization—should generalize naturally.

Finally, the computational complexity of our methods limits their applicability to large orders. For $n \geq 6$, even generating a single magic square by the Siamese method is trivial, but systematic exploration of the arrangement space becomes infeasible. Theoretical advances that predict properties of Magic Gems without exhaustive computation would significantly extend the reach of the framework.

5.8 Potential Applications

Beyond its intrinsic mathematical interest, the Magic Gem framework may have practical applications.

In education, the three-dimensional visualization of magic squares provides an accessible entry point to concepts from linear algebra, statistics, and geometry. The physical intuition of “balance” helps students understand why magic squares are special and motivates the algebraic constraints that define them.

In computational design, the covariance characterization could inform algorithms for constructing or recognizing magic squares. Gradient-descent methods minimizing off-diagonal co-

variance might provide an alternative to combinatorial search, though the non-convexity of the landscape poses challenges.

In recreational mathematics and art, Magic Gems offer a new way to visualize and appreciate magic squares. The polyhedra could be 3D-printed as physical objects, their shapes encoding the magic property in tangible form.

5.9 Algorithmic Implications

The energy landscape perspective suggests natural algorithmic strategies for magic square generation beyond classical backtracking. Since magic squares are isolated local minima, gradient-based descent in the $E_{\text{full}}(S)$ objective becomes viable. The challenge lies not in navigating a rugged landscape (entropy is modest, $H \approx 4.3\text{--}5.0$), but in the sheer breadth of the search space and the rarity of solutions.

Simulated annealing with the covariance energy as a temperature-dependent objective, or basin-hopping methods that leverage the isolation property, merit investigation. If the apparent quadratic scaling of peak energy is confirmed at larger orders, temperature schedules for such algorithms should also scale quadratically with order.

The isolation property (every swap increases energy) suggests that local search from a near-magic configuration could be effective—if such starting points can be found. Continuous relaxations of the discrete optimization problem, followed by projection onto the nearest permutation, offer another avenue enabled by the energy landscape framework.

6 Conclusion

We have introduced Magic Gems, a geometric framework for representing magic squares as three-dimensional polyhedra. This framework reveals deep connections between the classical algebraic definition of magic squares and concepts from statistics, optimization, and statistical mechanics, opening new avenues for understanding these ancient mathematical objects.

Our central theoretical contribution is the Complete Energy Characterization Theorem (Theorem 3.17), which establishes that an arrangement of integers in a square grid is a magic square if and only if its covariance with every row, column, and diagonal indicator vanishes. Equivalently, magic squares are precisely the ground states of the complete energy functional E_{full} , valid for all orders $n \geq 3$. This characterization transforms the discrete, combinatorial magic property into a statistical orthogonality condition with physical meaning.

The proof is elementary once the right framework is established: each row/column covariance vanishes if and only if that line sums to $M(n)$, and similarly for the diagonals. The perturbation analysis confirms that magic squares are isolated local minima, with every single-swap perturbation strictly increasing the energy.

We also investigated a natural simplification—the four-term “low-mode” energy using aggregate position coordinates X , Y and diagonal indicators. This characterizes magic squares for $n = 3$ (verified exhaustively), but defines a strictly larger class of “low-mode balanced” arrangements for $n \geq 4$. The existence of non-magic zeros of the low-mode energy, while initially surprising, follows from a dimensional argument: four linear constraints cannot determine all $2n$ line-sum conditions. Explicit counterexamples (Remark 3.10) and comparative energy analysis (Figure 4) illuminate this distinction, highlighting the necessity of the complete row/column indicator basis for a rigorous characterization.

The energy landscape perspective offers the most compelling conceptual insight. Magic squares are not merely configurations satisfying arithmetic constraints; they are equilibrium states where an imbalance energy vanishes. Like stones that have rolled to rest at the bottoms of valleys, magic squares occupy the deepest wells in a rugged terrain of arrangements. This view

connects magic squares to optimization theory, statistical mechanics, and dynamical systems, suggesting new algorithmic and theoretical approaches.

The Magic Gem framework opens several directions for future research. The geometric classification of magic squares, particularly for $n = 4$ where 880 essentially different squares exist, could complement traditional algebraic approaches. Extensions to magic hypercubes, semi-magic squares, and pandiagonal squares would test the generality of our framework. The “low-mode balanced” class identified by $E_{\text{low}} = 0$ for $n \geq 4$ is itself an interesting mathematical object worthy of further study.

The Lo Shu square has fascinated humanity for nearly five thousand years, its balanced arrangement of numbers inspiring mythology, art, and mathematics across cultures. By transforming this arrangement into a three-dimensional object—a gem that sits at the bottom of an energy well, whose very shape encodes perfect equilibrium—we hope to have added a new facet to its enduring mathematical beauty.

References

- [1] Maya M. Ahmed. How many squares are there, mr. Franklin?: Constructing and enumerating Franklin squares. *The American Mathematical Monthly*, 111(5):394–410, 2004.
- [2] Maya M. Ahmed, Jesús A. De Loera, and Raymond Hemmecke. Polyhedral cones of magic cubes and squares. In *Discrete and Computational Geometry*, volume 25 of *Algorithms and Combinatorics*, pages 25–41. Springer, 2003.
- [3] W. S. Andrews. *Magic Squares and Cubes*. Dover Publications, 2nd edition, 1960.
- [4] Alexander Barvinok. *A Course in Convexity*. Graduate Studies in Mathematics. American Mathematical Society, 2002.
- [5] Matthias Beck and Andrew van Herick. Enumeration of 4×4 magic squares. *Mathematics of Computation*, 80(273):617–621, 2011.
- [6] Matthias Beck and Thomas Zaslavsky. Inside-out polytopes. *Advances in Mathematics*, 205(1):134–162, 2006. MR 2254310.
- [7] Albrecht Dürer. Melencolia I, 1514. Engraving featuring a 4×4 magic square.
- [8] Peter D. Loly. 88.30 the invariance of the moment of inertia of magic squares. *The Mathematical Gazette*, 88(511):113–119, 2004.
- [9] Peter D. Loly. Franklin squares: A chapter in the scientific studies of magical squares. *Complex Systems*, 17(2):143–157, 2007.
- [10] Peter D. Loly, Ian Cameron, Walter Trump, and Daniel Schindel. Magic square spectra. *Linear Algebra and its Applications*, 430(10):2659–2680, 2009.
- [11] R. P. Nordgren. On properties of special magic square matrices. *Linear Algebra and its Applications*, 437(8):2009–2025, 2012.
- [12] R. P. Nordgren. Spectra of order-4 special magic squares. *Linear Algebra and its Applications*, 455:320–331, 2014.
- [13] Clifford A. Pickover. *The Zen of Magic Squares, Circles, and Stars*. Princeton University Press, 2002.
- [14] Walter Trump. Enumeration of magic squares. Available at <http://www.trump.de/magic-squares/>, 2012.

A Appendix: Technical Details

This appendix provides additional technical details supporting the main text, including a complete proof of the forward direction of the covariance characterization and discussion of the energy functional approach.

A.1 Proof Strategy Overview

The Complete Energy Characterization Theorem (Theorem 3.17) is established via two complementary approaches:

Forward Direction (Algebraic): Direct proof that magic squares have zero energy, following from the algebraic relationship between covariances and line sums.

Converse Direction: For the complete energy E_{full} , the converse follows directly from the row/column covariance characterization (Proposition 3.15, Proposition 3.12). For the low-mode energy E_{low} , the converse holds only for $n = 3$ (verified by exhaustive enumeration of all 362,880 arrangements).

A.2 Detailed Proof: Magic Implies Zero Covariance

We provide a complete proof of Proposition 3.6, showing that every magic square has vanishing row and column covariances.

Detailed Proof of Proposition 3.6. Let $S = (s_{ij})$ be an $n \times n$ magic square, and define coordinates as in Definition 3.1:

$$\begin{aligned} x_{ij} &= j - \frac{n-1}{2}, \\ y_{ij} &= \frac{n-1}{2} - i, \\ z_{ij} &= s_{ij} - \frac{n^2+1}{2}. \end{aligned}$$

Step 1: Verification that means vanish. For the x -coordinate, we compute

$$\bar{x} = \frac{1}{n^2} \sum_{i=0}^{n-1} \sum_{j=0}^{n-1} \left(j - \frac{n-1}{2} \right) = \frac{1}{n^2} \cdot n \sum_{j=0}^{n-1} \left(j - \frac{n-1}{2} \right).$$

Since $\sum_{j=0}^{n-1} j = n(n-1)/2$, we have

$$\sum_{j=0}^{n-1} \left(j - \frac{n-1}{2} \right) = \frac{n(n-1)}{2} - n \cdot \frac{n-1}{2} = 0,$$

establishing $\bar{x} = 0$. An identical argument shows $\bar{y} = 0$.

For the z -coordinate,

$$\bar{z} = \frac{1}{n^2} \sum_{i,j} \left(s_{ij} - \frac{n^2+1}{2} \right) = \frac{1}{n^2} \left(\sum_{i,j} s_{ij} - n^2 \cdot \frac{n^2+1}{2} \right).$$

Since S is a permutation of $\{1, \dots, n^2\}$, we have $\sum_{i,j} s_{ij} = n^2(n^2+1)/2$, yielding $\bar{z} = 0$.

Step 2: Expression for $\text{Cov}(X, Z)$. With zero means, the covariance is

$$\text{Cov}(X, Z) = \frac{1}{n^2} \sum_{i,j} x_{ij} z_{ij} = \frac{1}{n^2} \sum_{i,j} \left(j - \frac{n-1}{2} \right) \left(s_{ij} - \frac{n^2+1}{2} \right).$$

Expanding the product and separating terms:

$$\begin{aligned} n^2 \cdot \text{Cov}(X, Z) &= \sum_{i,j} j \cdot s_{ij} - \frac{n-1}{2} \sum_{i,j} s_{ij} \\ &\quad - \frac{n^2+1}{2} \sum_{i,j} j + \frac{(n-1)(n^2+1)}{4} n^2. \end{aligned}$$

We evaluate each term. First, $\sum_{i,j} s_{ij} = n^2(n^2+1)/2$. Second, $\sum_{i,j} j = n \sum_{j=0}^{n-1} j = n \cdot n(n-1)/2 = n^2(n-1)/2$. Substituting these and simplifying:

$$\begin{aligned} n^2 \cdot \text{Cov}(X, Z) &= \sum_{i,j} j \cdot s_{ij} - \frac{(n-1)n^2(n^2+1)}{4} - \frac{(n^2+1)n^2(n-1)}{4} + \frac{(n-1)(n^2+1)n^2}{4} \\ &= \sum_{i,j} j \cdot s_{ij} - \frac{(n-1)(n^2+1)n^2}{4}. \end{aligned}$$

Step 3: Connection to column sums. Let $C_j = \sum_{i=0}^{n-1} s_{ij}$ denote the sum of column j . Then

$$\sum_{i,j} j \cdot s_{ij} = \sum_{j=0}^{n-1} j \cdot C_j.$$

Since S is a magic square, all column sums equal $M(n) = n(n^2+1)/2$. Then

$$\sum_{j=0}^{n-1} j \cdot C_j = M(n) \sum_{j=0}^{n-1} j = \frac{n(n^2+1)}{2} \cdot \frac{n(n-1)}{2} = \frac{n^2(n-1)(n^2+1)}{4},$$

which exactly equals the second term above. Hence $\text{Cov}(X, Z) = 0$.

The argument for $\text{Cov}(Y, Z) = 0$ is entirely analogous, using row sums in place of column sums. \square

A.3 Why Row and Column Covariances Alone Are Insufficient

A natural question is whether the conditions $\text{Cov}(X, Z) = \text{Cov}(Y, Z) = 0$ alone characterize magic squares (or even semi-magic squares with equal row and column sums). The answer is negative, and understanding why is instructive.

Let $\delta_j = C_j - M(n)$ denote the deviation of column j from the magic sum. The constraint $\text{Cov}(X, Z) = 0$ is equivalent to $\sum_j (j - \frac{n-1}{2}) \delta_j = 0$. Combined with the total sum constraint $\sum_j \delta_j = 0$, this leaves an $(n-2)$ -dimensional space of possible deviation patterns.

For $n = 3$, the deviation pattern must be $(\delta_0, \delta_1, \delta_2) = t(1, -2, 1)$ for some t . While the $t = 0$ case corresponds to equal column sums, *non-zero values of t are achievable*: exhaustive enumeration reveals 128 arrangements with column sums $(16, 13, 16)$ (i.e., $t = 1$) that simultaneously satisfy $\text{Cov}(Y, Z) = 0$.

The total count is 760 arrangements with both $\text{Cov}(X, Z) = \text{Cov}(Y, Z) = 0$, of which only 8 are magic squares. The remaining 752 arrangements satisfy the row and column covariance conditions but fail to achieve equal row sums, equal column sums, or the diagonal conditions.

A.4 Complete vs. Low-Mode Energy Characterization

The main text establishes two energy functionals with different characterization properties.

A.4.1 Complete Energy (Theorem)

The *complete magic energy* uses individual row and column indicator covariances:

$$E_{\text{full}}(S) = \sum_{k=0}^{n-2} \text{Cov}(R_k, Z)^2 + \sum_{\ell=0}^{n-2} \text{Cov}(C_\ell, Z)^2 + \text{Cov}(D_{\text{main}}, Z)^2 + \text{Cov}(D_{\text{anti}}, Z)^2, \quad (17)$$

where $R_k(i, j) = \mathbf{1}\{i = k\}$ and $C_\ell(i, j) = \mathbf{1}\{j = \ell\}$.

Theorem A.1 (Complete Energy Characterization—All n). *For all $n \geq 3$, an arrangement S of $\{1, 2, \dots, n^2\}$ in an $n \times n$ grid is a magic square if and only if $E_{\text{full}}(S) = 0$.*

This is proven in Theorem 3.17 of the main text. The proof follows directly from the row/column covariance characterization: each row covariance vanishes iff that row sums to $M(n)$, each column covariance vanishes iff that column sums to $M(n)$, and each diagonal covariance vanishes iff that diagonal sums to $M(n)$.

A.4.2 Low-Mode Energy (Partial Characterization)

The simpler *low-mode energy* uses aggregate position coordinates:

$$E_{\text{low}}(S) = \text{Cov}(X, Z)^2 + \text{Cov}(Y, Z)^2 + \text{Cov}(D_{\text{main}}, Z)^2 + \text{Cov}(D_{\text{anti}}, Z)^2. \quad (18)$$

For $n = 3$: Exhaustive enumeration confirms that $E_{\text{low}}(S) = 0$ if and only if S is a magic square. Exactly 8 of 362,880 arrangements achieve zero energy, all being the Lo Shu and its D_4 symmetry variants.

For $n \geq 4$: The condition $E_{\text{low}}(S) = 0$ defines a *strictly larger* class of “low-mode balanced” arrangements that properly contains the magic squares. Counterexamples exist: for example, the 4×4 arrangement

$$\begin{pmatrix} 9 & 4 & 12 & 3 \\ 16 & 1 & 14 & 7 \\ 10 & 15 & 11 & 8 \\ 2 & 5 & 6 & 13 \end{pmatrix}$$

has $E_{\text{low}}(S) = 0$ (both diagonals sum to 34, and the first-moment conditions are satisfied), but row sums (28, 38, 44, 26) and column sums (37, 25, 43, 31) are not equal. This demonstrates that the four-term energy is insufficient for $n \geq 4$.

Why random sampling failed to detect counterexamples: The probability of a uniformly random permutation achieving $E_{\text{low}} = 0$ is extremely low (estimated below 10^{-8} for $n = 4$), so 460 million samples are unlikely to encounter such configurations. However, targeted search methods (e.g., hill-climbing on the constraint residuals) readily find them. This illustrates a fundamental limitation of random sampling for disproving “if and only if” conjectures.

A.5 Computational Methods

All computations were performed in Python 3 using the NumPy and SciPy libraries for numerical computation and the Matplotlib library for visualization. Convex hulls were computed using SciPy’s implementation of the Quickhull algorithm.

Random arrangements were generated by applying the Fisher-Yates shuffle to the array $[1, 2, \dots, n^2]$ and reshaping to an $n \times n$ grid. This procedure samples uniformly from the $n^2!$ possible arrangements.

Magic squares were generated using classical construction methods: the Siamese (de la Loubère) method for odd orders ($n = 3, 5$) and the doubly-even diagonal method for $n = 4$. This choice of methods ensures that we test the framework across both parity classes, which differ in their geometric structure (presence or absence of a central cell) and construction algorithms. The zero-covariance property was verified to hold within floating-point precision (typically $< 10^{-14}$) for all generated magic squares of all three orders.

Source code for all analyses and figures is available in the supplementary materials. An interactive web application for visualizing Magic Gems is available at <https://kylemath.github.io/MagicGemWebpage/>.

A.6 Summary Statistics

Table 4 summarizes key statistics for magic squares of orders 3, 4, and 5.

n	Arrangements	Magic Squares	Equiv. Classes	Probability	$M(n)$
3	3.6×10^5	8	1	2.2×10^{-5}	15
4	2.1×10^{13}	7,040	880	3.4×10^{-10}	34
5	1.6×10^{25}	2.8×10^8	3.4×10^7	1.8×10^{-17}	65

Table 4: Statistics for magic squares of orders 3, 4, and 5, showing the total number of arrangements, number of magic squares, number of equivalence classes under D_4 , probability of a random arrangement being magic, and the magic constant $M(n)$.